Immunology and Inflammation
Microbiology and Infectious Disease

SARS-CoV-2 nsp16 is regulated by host E3 ubiquitin ligases, UBR5, and MARCHF7

Reviewed Preprint
v2 • March 24, 2025
Revised by authors

Reviewed Preprint
v1 • December 24, 2024

Li Tian, Zongzheng Zhao, Wenying Gao, Zirui Liu, Xiao Li, Wenyan Zhang, Zhaolong Li

Department of Infectious Diseases, Infectious Diseases and Pathogen Biology Center, Institute of Virology and AIDS Research, Key Laboratory of Organ Regeneration and Transplantation of The Ministry of Education, The First Hospital of Jilin University, Changchun, China • Research Unit of Key Technologies for Prevention and Control of Virus Zoonoses, Chinese Academy of Medical Sciences, Changchun Veterinary Research Institute, Chinese Academy of Agricultural Sciences, Changchun, China

eLife Assessment

This **important** work advances our understanding of how the SARS-CoV-2 Nsp16 protein is regulated by host E3 ligases to promote viral mRNA capping. Support for the overall claims in the revised manuscript is **convincing** . This work will be of interest to those working in host-viral interactions and the role of the ubiquitin-proteasome system in viral replication.

https://doi.org/10.7554/eLife.102277.2.sa3

Abstract

Severe acute respiratory syndrome coronavirus 2 (SARS-CoV-2), the virus responsible for coronavirus disease 2019 (COVID-19), remains a global public health threat with major economic implications. The non-structural protein 16 (nsp16) of SARS-CoV-2, in complex with nsp10, catalyses the final step of viral mRNA capping via its 2'-O-methylase activity, enabling the virus to evade host immunity and protect viral mRNA from degradation. However, host factors regulating nsp16 have not been thoroughly explored. Although various E3 ubiquitin ligases are known to interact with SARS-CoV-2 proteins, their specific roles in targeting nsp16 for degradation remain unclear. In this study, we demonstrate that nsp16 is ubiquitinated and degraded by host E3 ubiquitin ligases UBR5 and MARCHF7, acting through the ubiquitin-proteasome system (UPS). UBR5 and MARCHF7 induce nsp16 degradation via K48- and K27-linked ubiquitination, respectively, in independent processes that inhibit SARS-CoV-2 replication both in vitro and in vivo. Furthermore, UBR5 and MARCHF7 exhibited broad-spectrum antiviral activity by degrading nsp16 variants from different SARS-CoV-2 strains. Our findings uncover novel mechanisms by which the UPS antagonises SARS-CoV-2 replication and provide promising targets for therapeutic intervention against COVID-19.

Introduction

Severe acute respiratory syndrome coronavirus 2 (SARS-CoV-2) has emerged as a global public health threat, causing over 700 million coronavirus disease 2019 (COVID-19) cases and 7 million deaths (Carabelli et al., 2023; Markov et al., 2023). SARS-CoV-2 encodes four structural proteins, 16 non-structural proteins (Nsps) that assist in viral replication and transcription, and a series of accessory proteins (ORFs) associated with immune evasion (V'kovski et al., 2021; Wang et al., 2020). Some viruses such as Ebola virus (Valle et al., 2021), dengue virus (Jung et al., 2018), and reovirus (Furuichi et al., 1975) encode 2'-O methyltransferases (2'-O-MTases) homologous to those found in eukaryotes. This allows them to mimic the host 5' cap structure on their RNA, hindering recognition by the innate immune system (Daffis et al., 2010; Züst et al., 2011). Similarly, SARS-CoV-2 nsp16, in complex with nsp10, functions as a 2'-O-MTase, methylating the first nucleotide of a capped viral RNA strand at the 2'-O position, converting the 5' cap of RNA from 'cap-0' to 'cap-1' (Benoni et al., 2021; Park et al., 2022). This modification shields SARS-CoV-2 from host antiviral responses such as MDA5 recognition and IFIT1 restriction (Bergant et al., 2022; Russ et al., 2022). Importantly, nsp16 inhibits global host mRNA splicing, which reduces host protein and mRNA levels (Banerjee et al., 2020). Additionally, nsp16 enhances SARS-CoV-2 cell entry by promoting TMPRSS2 expression (Han et al., 2023), highlighting its multifaceted role as a virulence factor. Moreover, nsp16-deficient strains exhibit reduced pathogenicity and induce a strong immune response, suggesting their potential as a live-attenuated vaccine candidate (Ye et al., 2022). Given nsp16's critical functions, drugs targeting nsp16 or the nsp16-nsp10 complex have been developed (Klima et al., 2022; Nguyen et al., 2022). Therefore, understanding host factors that interact with nsp16 is crucial for uncovering novel therapeutic strategies.

The ubiquitin-proteasome system (UPS) is an important pathway for the targeted degradation of intracellular proteins and is referred to as "the molecular kiss of death" (Dongdem & Wezena, 2021; Park et al., 2020). Substrate ubiquitination requires a cascade of three ligases: E1, E2, and E3 (Zheng & Shabek, 2017). Some E3 ubiquitin ligases function as monomers, while others form multi-subunit E3 complexes. Regardless of their form, all E3 ligases share the same functional specificity in recognizing substrates and determining the specificity of the UPS. In some complexes, an additional protein may be required as a substrate receptor to recognize the substrate (Iconomou & Saunders, 2016; Yang et al., 2021). E3 ligases are indispensable for direct binding to substrates and determining the specificity of the UPS (Li et al., 2021; Wang et al., 2022). Researchers have identified over 600 human genome-encoded E3 ligases that operate in diverse cellular environments, respond to a wide range of cellular signals, and regulate a vast array of protein substrates (Dongdem & Wezena, 2021; Garcia-Barcena et al., 2020). Dysregulation of E3 ligase activity has been implicated in various human diseases, making them promising drug targets (Humphreys et al., 2021). E3 ligases are classified into three classes based on conserved domains and ubiquitin (Ub) transfer mechanisms: Really Interesting New Gene (RING) E3s, homologous to the E6AP carboxyl terminus (HECT) E3s, and RING-between-RING (RBR) E3s (Garcia-Barcena et al., 2020; Morreale & Walden, 2016). RING E3 ligases directly transfer Ub from the E2-Ub complex to the substrate (Deshaies & Joazeiro, 2009), whereas HECT-type E3s transfer Ub to their own catalytic cystine residue before attaching it to the substrate (Huibregtse et al., 1995). RBR E3s combine the characteristics of both RING and HECT types (Walden & Rittinger, 2018). RBR and RING E3s share the RING-binding domains, but RBR family members can generate thioester intermediates with Ub, as is the case with HECT-type E3s (Garcia-Barcena et al., 2020).

To investigate the relationship between SARS-CoV-2 and host factors, we focused on the interaction between nsp16 and the UPS. In this study, we present a novel regulatory mechanism targeting nsp16 via the host UPS. We demonstrate, for the first time, that nsp16 is ubiquitinated and degraded by the host proteasome. Interestingly, two E3 ligases from distinct families, the RING-type MARCHF7 and the HECT-type UBR5, independently recognise and target nsp16 for

degradation in the cytoplasm and nucleus. Since nsp16 possesses 2'-O-MTase activity, its enzymatic function converts the viral RNA 5' cap structure from cap-0 to cap-1. This dual targeting of nsp16 by MARCHF7 and UBR5 leads to its degradation, disrupting its function and ultimately demonstrating effective antiviral activity against SARS-CoV-2. Our findings identify novel therapeutic targets for developing effective strategies to prevent SARS-CoV-2 and treat COVID-19.

Results

Ubiquitination and proteasomal degradation of SARS-CoV-2 nsp16 by the UPS

Ubiquitination plays an important role in SARS-CoV-2 infection and pathogenesis (Gao et al., 2022; Guo et al., 2021; Li et al., 2023; Zhang et al., 2021; Zhang et al., 2024; Zhang et al., 2023). To explore whether the non-structural proteins of SARS-CoV-2 are regulated by the UPS, we examined the effect of the proteasome inhibitor MG132 on the protein expression of all 16 non-structural proteins. MG132 treatment markedly increased the abundance of nsp8, nsp11, and nsp16 proteins in HEK293T cells (**Fig. 1A**), suggesting their potential degradation by the UPS. It has been reported that nsp8 undergoes UPS-mediated degradation via TRIM22-mediated ubiquitination (Fan et al., 2024). In this study, we focused on nsp16 for further investigation. To confirm the role of the UPS in nsp16 degradation, we employed additional proteasome inhibitors, Bortezomib and Carfilzomib. Unlike the lysosomal inhibitors Bafilomycin A1 and NH_4Cl and the autophagy-lysosomal inhibitor vinblastine, these proteasome inhibitors enhanced nsp16 stability (**Fig. 1B**). The impact of the USP on the half-life of nsp16 was investigated. To this end, nsp16-expressing cells were treated with a protein synthesis inhibitor, cycloheximide, and the kinetics of nsp16 decay were examined. We observed that the half-life of nsp16 in MG132-treated samples was significantly longer than that in MG132-untreated samples (15 h versus 2 h) (**Fig. 1C** and **1D**).

To identify proteins interacting with nsp16, we performed co-immunoprecipitation (Co-IP) followed by mass spectrometry (MS) analysis, comparing nsp16-expressing cells treated with and without MG132 (**Fig. 1E**). KEGG pathway and Gene Ontology analyses of the MS data (**Figure 1—figure supplement 1A**). Biological process enrichment analysis showed that blocking nsp16 degradation resulted in an increase in the number of proteins that interact with it, including 43 proteins involved in virus-associated processes and 22 proteins involved in regulating mRNA stability. Five proteins were related to the regulation of the cellular antiviral defence. Additionally, interactions were associated with mRNA splicing and RNA methylation (Banerjee et al., 2020), consistent with nsp16's role as a 2'-O-MTase. Furthermore, SARS-CoV-2 uses nsp16 to disrupt host mRNA splicing to facilitate its infection (Park et al., 2022; Russ et al., 2022; Züst et al., 2011). These findings corroborate the reliability of our MS data.

As expected, we found that several nsp16-binding proteins were related to ubiquitination and degradation pathways (**Figure 1 — figure supplement 1B**). Four deubiquitinases (DUBs), the E2 ligase UBE2D3, and 14 proteasomal enzymes were identified. Of these, six E3 ligases, UBR5, MARCHF7, HECTD1, TRIM32, MYCBP2, and TRIM21, were chosen for further investigation.

E3 ligases UBR5 and MARCHF7 independently mediate nsp16 degradation

To identify the E3 ligases responsible for nsp16 degradation, we designed small interfering RNA (siRNA) targeting the six candidate E3 ligases and evaluated their effects on nsp16 abundance. Knockdown of UBR5 and MARCHF7 stabilised the protein levels of nsp16 (**Fig. 2A**). Furthermore, we generated stable cell lines with UBR5 or MARCHF7 knockdowns to further investigate their effects on nsp16 stability and confirm silencing efficiency (**Fig. 2B**). To determine whether UBR5

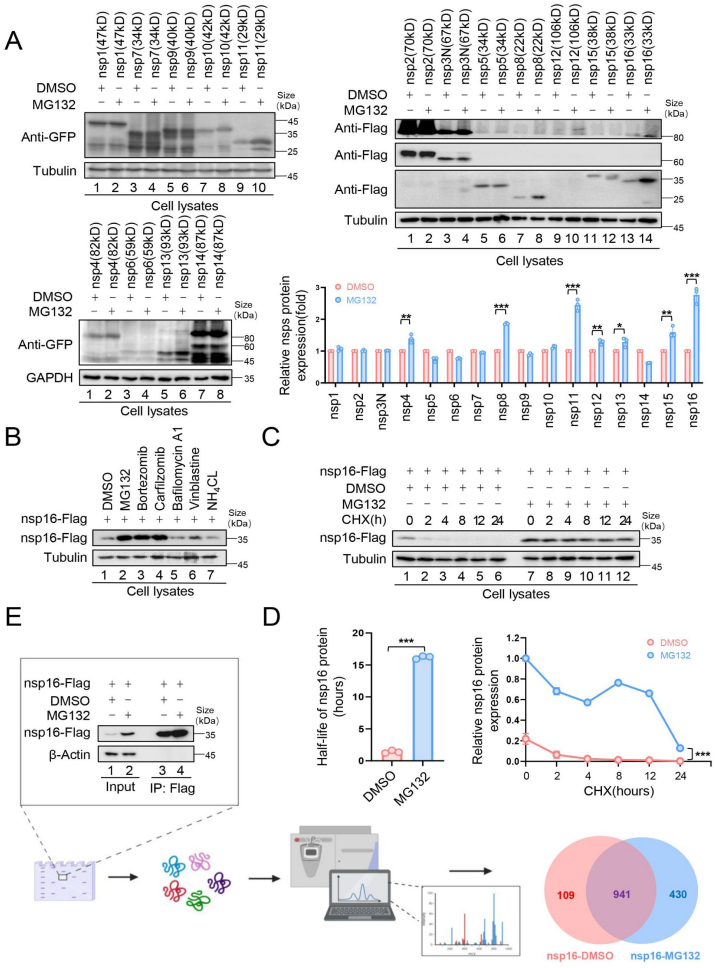

Figure 1.

The non-structural protein nsp16 of SARS-CoV-2 was identified that can be degraded through the proteasome pathway.

A. The non-structural proteins nsp8, nsp11 and nsp16 could be restored by the proteasome inhibitor MG132. HEK293T cells in 12-well plates were transfected with the plasmids of 16 nonstructural proteins (nsp1-16) encoded by SARS-CoV-2. Thirty-six hours later, the cells were treated with MG132 (10 μM) or DMSO for 12 h before collection. The protein level was detected by Immunoblotting (IB). Quantification of nsp protein levels relative to the control protein is shown. Data are representative of three independent experiments and shown as average ±SD (n = 3). Significance was determined by a two-tailed t-test: *P < 0.05; **P < 0.01; ***P < 0.001. B. Proteasomal inhibitors but no other inhibitors stabilized nsp16 protein. HEK293T cells transfected with the nsp16-Flag expression vector were treated with dimethyl sulfoxide (DMSO), MG132 (10 μM), Bortezomib (10 μM), Carfilzomib (10 μM), Bafilomycin A1 (5 μM), Vinblastine (2.5 μM), or NH_4CL (2.5 μM) for 12 h prior to harvest. The cell lysates were analyzed by anti-Flag antibody. (C-D). The half-life of nsp16 was prolonged by the proteasome inhibitor MG132. C. HEK293T cells were transfected with the nsp16-Flag-expressing plasmids. 12 hours later, the cells were treated with DMSO or MG132 (10 μM) for 12 h, then 50 μg/mL cycloheximide (CHX) was added. Cells were harvested at the indicated times to detect the level of viral protein by anti-Flag antibody. D. Quantification of nsp16 protein levels relative to tubulin at different time points is shown. The half-life of the nsp16 protein was determined based on protein quantification using Image J, combined with the protein half-life formula for calculation. Results are shown as mean ± SD (n = 3 independent experiments). ***, P < 0.001 by by a two-tailed t-test.

E. Samples were prepared for mass spectrometry, and nsp16 interacting proteins were obtained by immunoprecipitation (IP) (created using *BioRender.com*). The plasmids were transfected into HEK293T cells for 48 h. Treat cells with or without MG132 (10 μM) for 12 h prior to harvest. The whole-cell lysates were incubated with protein G agarose beads conjugated with anti-Flag antibodies and used for IB with anti-Flag antibodies to detect the nsp16 protein. Samples enriched for proteins were analyzed by mass spectrometry.

and MARCHF7 cooperate in nsp16 degradation, we knocked down UBR5 or MARCHF7 using siRNA in MARCHF7- or UBR5-knockdown cells, respectively. Knockdown of UBR5 in MARCHF7-knockdown cells, and vice versa, further enhanced nsp16 stability. This indicates that UBR5 and MARCHF7 act independently to degrade nsp16 (**Fig. 2C**). We further validated the independent function of these E3 ligases by examining nsp16 degradation. MARCHF7 overexpression induced nsp16 degradation in both MARCHF7-knockdown and MARCHF7/UBR5-double-knockdown cells. Similarly, UBR5 overexpression degraded nsp16 even in the presence of MARCHF7 knockdown. Knockdown efficiencies were confirmed for all experiments (**Figure 2 — figure supplement 1A** and 1B). Notably, overexpression of wild-type MARCHF7 or UBR5, but not mutants lacking the functional RING domain (1-542 aa) or the HECT domain inactivated mutant, disrupts the stability of nsp16 in cells with MARCHF7 or UBR5 knockdown (**Fig. 2D** and **2E**). These findings demonstrate that UBR5 and MARCHF7 independently ubiquitinate nsp16 via their HECT or RING domains, targeting it for proteasomal degradation.

UBR5 and MARCHF7 mediate distinct Ub linkages on nsp16

We first confirmed the ubiquitination of nsp16, both in the presence and absence of exogenous Ub (**Fig. 3A-B**). To further investigate the regulation by E3 ligases, we examined the impact of UBR5 or MARCH7 knockdown on nsp16 ubiquitination. Knockdown of either UBR5 or MARCHF7 decreased the ubiquitination level of nsp16 compared to that in the negative control (**Fig. 3C**). Ub contains seven lysine residues (K6, K11, K27, K29, K33, K49, and K63) that form polyubiquitin chains with distinct functions, ultimately dictating the fate of the attached target protein (Grice & Nathan, 2016). To determine the specific type of polyubiquitin chain modification of nsp16 mediated by UBR5 and MARCH7, we constructed a series of Ub mutants retaining only a single lysine residue. Except for K33, all single-lysine Ub mutants promoted nsp16 ubiquitylation to varying extents, suggesting a complex polyubiquitin chain structure on nsp16 potentially regulated by multiple E3 ligases or E2-E3 ligase pairs (**Fig. 3D**). Notably, analysis of specific lysine linkages revealed that MARCHF7 knockdown primarily reduced the K27-linked ubiquitination of nsp16, while UBR5 knockdown primarily reduced the K48-linked ubiquitination of nsp16 (**Fig. 3E** and **3F**). These findings indicate that MARCHF7 and UBR5 induce K27- and K48-linked ubiquitination on nsp16, respectively.

UBR5 and MARCHF7 directly interact and colocalise with nsp16 in the endoplasmic reticulum (ER)

MS analysis suggested interactions between nsp16 and both UBR5 and MARCH7. Co-IP experiments confirmed that both Myc-tagged MARCHF7 and endogenous UBR5 interact with nsp16 (**Figure 4 — figure supplement 1A** and 1B). To determine whether MARCHF7 or UBR5 directly interact with nsp16, fluorescence resonance energy transfer (FRET) assays were performed. When nsp16-YFP was bleached, the fluorescence signals from CFP-UBR5 or CFP-MARCHF7 fusion proteins increased, indicating a direct interaction between these E3 ligases and nsp16 (**Figure 4—figure supplement 1C**). Image J software was used to quantify the relative fluorescence intensities (**Figure 4 — figure supplement 1D**). We next investigated whether UBR5 and MARCHF7 require each other for nps16 binding. We compared the binding ability of UBR5 to nsp16 in the presence or absence of MARCHF7 using Co-IP. MARCHF7 knockdown had no effect on the interaction between UBR5 and nsp16, and vice versa (**Fig. 4A** and **4B**), indicating independent binding of UBR5 and MARCHF7 to nsp16. Previous studies have shown that nsp16 is localised to both the nucleus and cytoplasm (Zhang et al., 2020). UBR5 (containing two nuclear localisation signals) and MARCHF7 are present in both compartments (Muñoz-Escobar et al., 2015; Shearer et al., 2018) (Nathan et al., 2008). Immunofluorescence staining revealed that UBR5 and MARCHF7 colocalised primarily with nsp16 in the cytoplasm, with some colocalisation

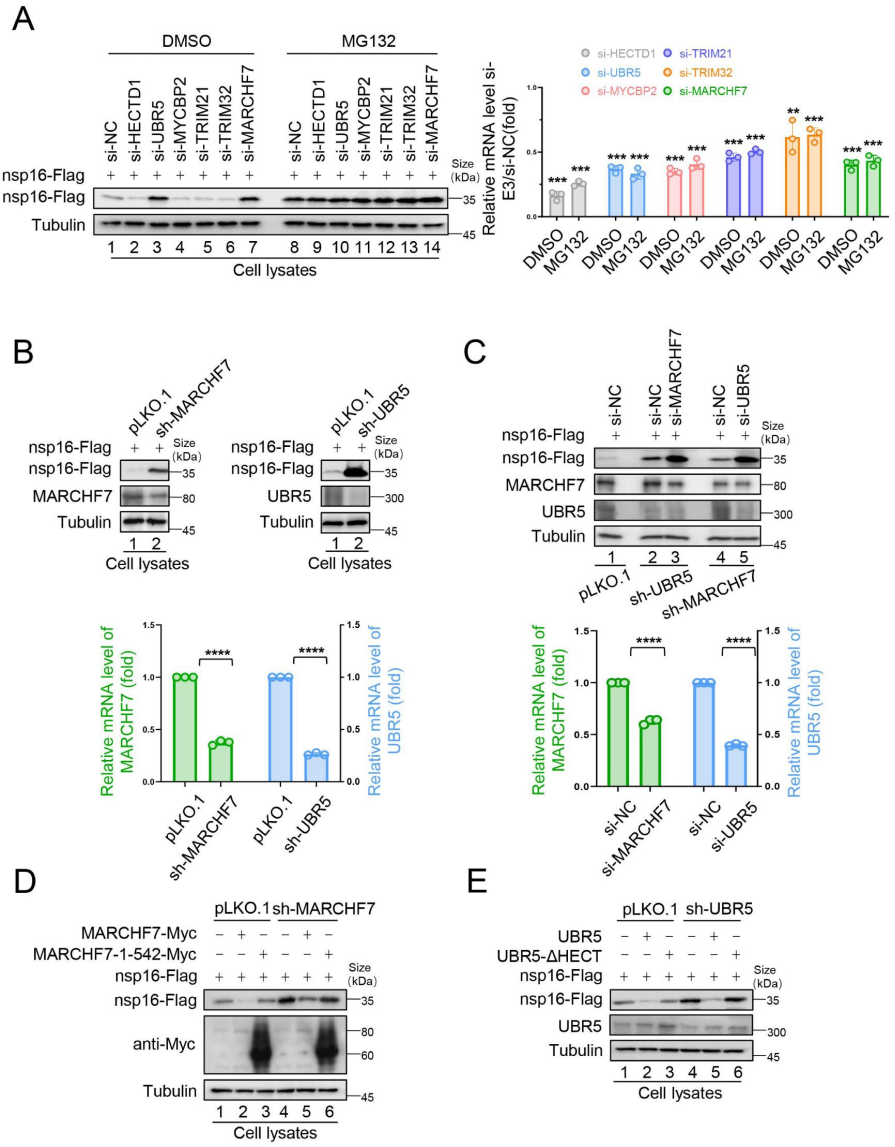

Figure 2.

MARCHF7 and UBR5 were identified as E3 ubiquitin ligases involves in nsp16 protein degradation.

A. Knockdown of MARCHF7 or UBR5 resulted in nsp16 restoration. HEK293T cells were transfected with siRNA of E3 ligase candidates for 24 h, followed by co-incubation with the nsp16-Flag-expressing plasmids for 48 h, treated with MG132 (10 μM) for 16h before harvesting, lysed, and subjected to IB assay using anti-Flag antibody. RT-qPCR was conducted to determine the mRNA expression levels of E3 ligase candidates. The si-RNA targeting regions for the candidate E3 ubiquitin ligase proteins and the targeted regions for RT-qPCR are shown in Appendix-figure S1A. Data are representative of three independent experiments and shown as average ± SD (n = 3). Significance was determined by a two-tailed t-test: ***P < 0.001.

B. RNA levels of UBR5 or MARCHF7 from HEK293T cells infected with lentivirus containing control or shRNA targeting UBR5 or MARCHF7 for 48 h and screened with antibiotics for 48 h. Knockdown cell lines were transfected with plasmids expressing nsp16-Flag, collected at the indicated times, and the protein levels of nsp16, MARCHF7, and UBR5 were detected by IB.C. MARCHF7 and UBR5 acted separately and did not depend on each other. HEK293T cells stably expressing UBR5 shRNA or MARCHF7 shRNA were transfected with siRNA of MARCHF7 or UBR5 for 24 h, respectively, followed by co-incubation with the nsp16-Flag-expressing plasmids for 48 h. The protein levels and the RNA levels of nsp16, UBR5 and MARCHF7 were measured by IB and RT-qPCR, respectively.

(D-E). In HEK293T cells stably expressing UBR5 shRNA or MARCHF7 shRNA, nsp16 was degraded by overexpressed UBR5 or MARCHF7, respectively, whereas the mutant failed to degrade nsp16. The cell lysates were analyzed by anti-Flag antibody.

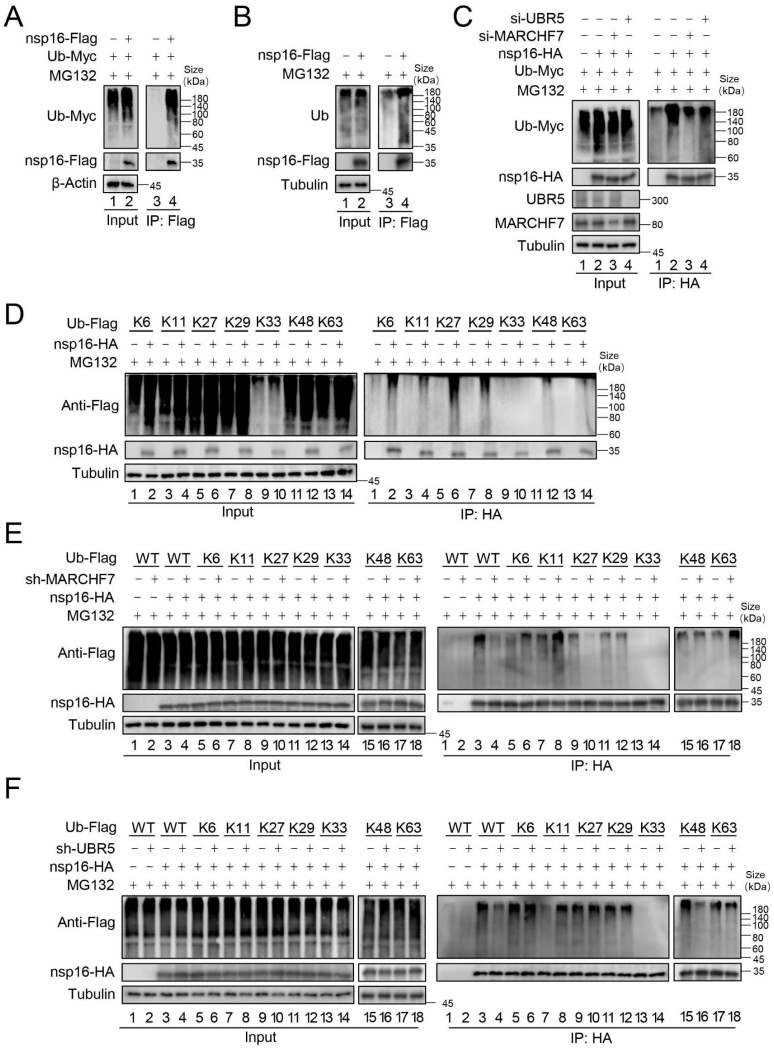

Figure 3.

MARCHF7 or UBR5 catalyze the formation of K-27 type or K-48 type ubiquitin chains of nsp16 respectively.

A. Nsp16 can be ubiquitinated. HEK293T cells co-transfected with ubiquitin-Myc and nsp16-Flag or transfected with nsp16-Flag alone. The cells were treated with MG132 for 12 h before collection. The whole-cell lysates were incubated with anti-Flag beads and used for IB with anti-Myc or anti-Flag antibodies to detect the polyubiquitination chain of nsp16.
B. Assess the endogenous ubiquitination level of nsp16 protein. Cells were transfected with nsp16-Flag or an empty vector, and collected 48 hours later. Prior to harvesting, cells were treated with MG132 for 16 hours. Co-IP experiments were then performed to analyze the endogenous ubiquitination level of nsp16.
C. The level of ubiquitination of nsp16 decreased with decreasing the protein levels of MARCHF7 or UBR5. E3 was knocked down by transfection with siRNA targeting UBR5 or MARCHF7, and 24 h later ubiquitin-Myc and nsp16-HA were co-transfected or nsp16-HA alone. Cells were treated with MG132 for 16 h before collection. Whole cell lysates were incubated with anti-HA beads, and polyubiquitinated chains of nsp16 were detected by IB with anti-Myc or anti-HA antibodies.
D. Nsp16 can be modified by a variety of ubiquitin chains. HEK293T cells were transfected with either nsp16-HA alone or together with plasmids encoding various mutants of ubiquitin (K6 only, K11 only, K27 only, K29 only, K33 only, K48 only, K63 only). Thirty-six hours later, cells were treated with MG132 for 12 h. Cell lysates were then subjected to immunoprecipitation, followed by IB to analysis.
(E-F) MARCHF7 or UBR5 causes nsp16 to be modified by the K27 type or K48 type ubiquitin chain. 293T cell lines with or without MARCHF7 or UBR5 knockdown were co-transfected with plasmids encoding ubiquitin-WT or various mutants of ubiquitin (K6 only, K11 only, K27 only, K29 only, K33 only, K48 only, K63 only). The other experimental methods were the same as C.

in the nucleus of Hela cells (**Figure 4—figure supplement 1E**). Similar results were observed in nsp16-transfected HEK293T cells using antibodies against endogenous UBR5 or MARCHF7 (**Figure 4 — figure supplement 1F**).

To identify the specific cellular compartment where UBR5 or MARCH7 interacts with nsp16, we co-transfected cells with UBR5-CFP or MARCH7-CFP along with nsp16-YFP. Immunostaining was performed with organelle-specific antibodies to label the mitochondrial marker COX5A, the ER marker PDI, and the Golgi apparatus marker GM130. Notably, both UBR5 and MARCHF7 interacted with nsp16 and colocalised with PDI, but not with COX5A or GM130 (**Fig. 4C** and **4D**). These findings indicate that UBR5 and MARCHF7 directly interact with nsp16 in the ER.

Functional domains of UBR5 and MARCHF7 are required for nsp16 interaction and ubiquitination

UBR5 is a four-domain E3 ligase containing two nuclear localisation signals. The four domains are UBA, UBR, PABC, and HECT (Muñoz-Escobar et al., 2015) (**Figure 4—figure supplement 2A**). Notably, the HECT domain is essential for its E3 ligase activity, where UBR5 must be conjugated to Ub before transferring it to the substrate (Kim et al., 2021).

To identify the UBR5 domain responsible for nsp16 ubiquitination, we utilised UBR5 mutants with inactivated individual domains. Only the HECT domain mutant failed to degrade nsp16 (**Figure 4—figure supplement 2B**), consistent with previous findings (Zhou et al., 2022), and was unable to induce nsp16 ubiquitination, further supporting its essential function (**Figure 4—figure supplement 2C**).

To identify the MARCHF7 region responsible for nsp16 degradation, we constructed a series of truncation mutants, as previously described (**Figure 4 — figure supplement 2D**) (Zhao et al., 2018) (Nathan et al., 2008). All mutants lost the ability to degrade nsp16 (**Figure 4—figure supplement 2E**). Furthermore, we explored the ability of these mutants to interact with nsp16 and their impact on nsp16 ubiquitination. Only the mutant with an intact N-terminal region (aa 1–542) retained strong binding to nsp16, while mutants with the active RING domain region (aa 543–616) did not. Consistently, only the wild-type MARCHF7 induced the formation of K27-linked Ub chains on nsp16 (**Figure 4 — figure supplement 2F**). These findings suggest that the N-terminal of MARCH7 mediates binding to nsp16, while the RING domain is required for its K27-linked ubiquitination activity.

UBR5 and MARCHF7 mediate antiviral activity against SARS-CoV-2 by targeting nsp16 for degradation

To examine the functional impact of nsp16 degradation by UBR5 and MARCHF7 on viral replication, we used a biosafety level 2 cell culture system to generate SARS-CoV-2 transmissible virus-like particles capable of infecting and replicating in Caco2-N^{int} cells (Ju et al., 2021). Knockdown of either UBR5 or MARCHF7 in these cells significantly increased SARS-CoV-2 replication compared with that in the control group. Notably, simultaneous knockdown of both UBR5 and MARCHF7 further increased SARS-CoV-2 replication (**Figure 5—figure supplement 1A** and 1B).

Given the critical antiviral roles of UBR5 and MARCH7, we investigated the modification of nsp16 following viral infection. HEK293T cells stably expressing the SARS-CoV-2 entry receptor ACE2 (HEK293T-ACE2) were infected with the Wuhan strain for 48 h. Co-IP using an anti-nsp16 antibody revealed that nsp16 interacts with endogenous MARCHF7 and UBR5 and undergoes ubiquitination (**Fig. 5A**). We further validated the antiviral effects of UBR5 and MARCH7 in a biosafety level 3 facility using the Wuhan strain at a multiplicity of infection (MOI) of 0.01 and the Omicron strain at an MOI of 0.001. Compared to the control group, UBR5 or MARCH7 knockdown in Caco2 cells

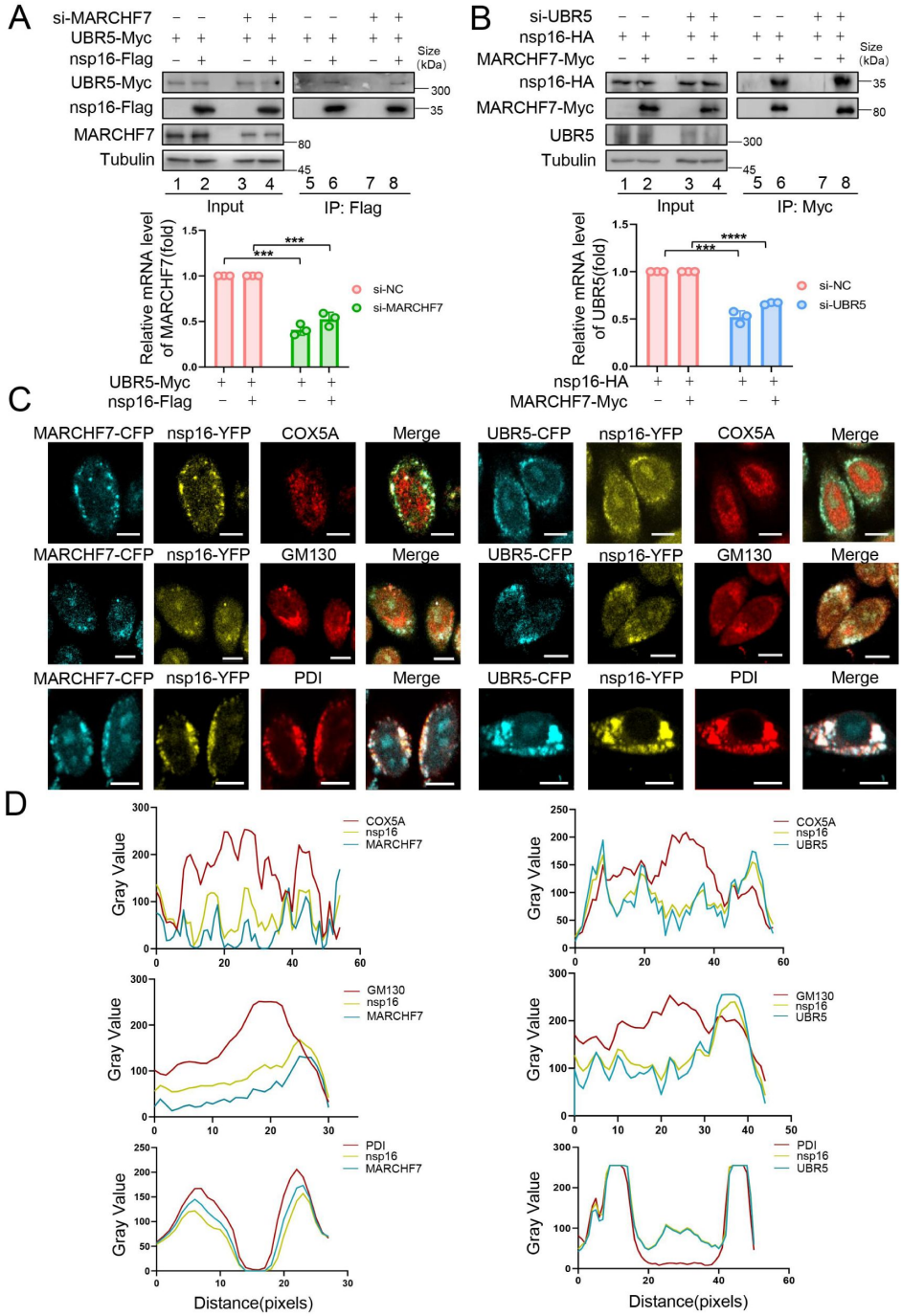

Figure 4.

MARCHF7 and UBR5 directly interact with nsp16 respectively.

(A-B). The binding of MARCHF7 or UBR5 to nsp16 was not mutually dependent. The binding of nsp16 to UBR5 or MARCHF7 was identified by co-immunoprecipitation in HEK293T cells transfected siMARCHF7 or siUBR5, respectively. The immunoprecipitates and input were analyzed by IB. The knockdown efficiency was detected by RT-qPCR and IB.
(C-D). MARCHF7 or UBR5 co-localized with nsp16 in the endoplasmic reticulum. Hela cells were co-transfected with YFP-nsp16(yellow) and CFP-UBR5(cyan) or CFP-MARCHF7(cyan). The organelles were labeled with antibodies against marker proteins of endoplasmic reticulum, Golgi apparatus and mitochondria respectively(red). The cells were analyzed by confocal microscopy (C). Scale bars, 20 um. The ratio of colocalization was quantified by measuring the fluorescence intensities using Image J (D).

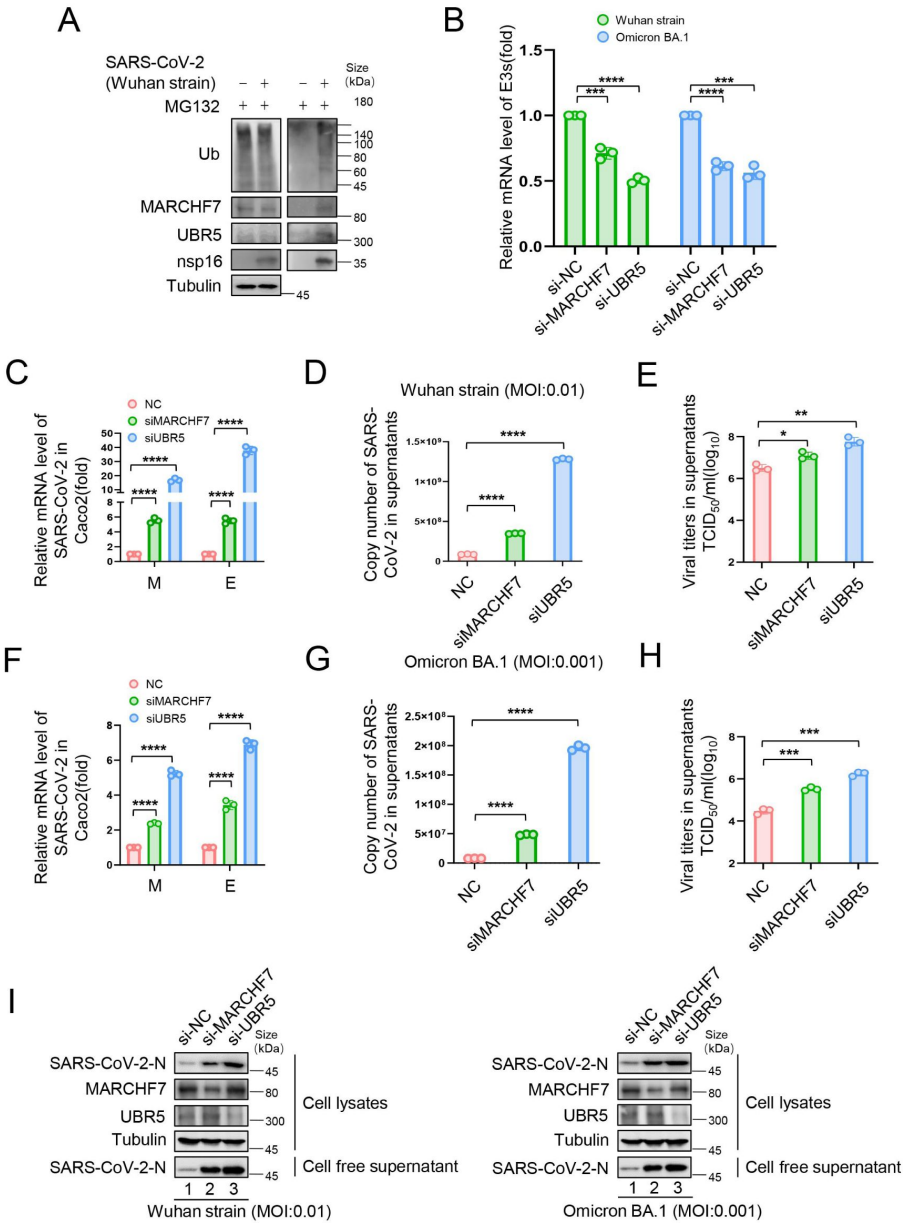

Figure 5.

Knockdown of MARCHF7 or UBR5 promotes viral replication.

A. The virus-encoded nsp16 protein interacts with endogenous MARCHF7 and UBR5 and undergoes ubiquitination modification. In 293T-ACE2 cells, with or without Wuhan strain infection (MOI: 0.01), the medium was changed 2 hours post-infection, and cells were harvested 48 hours later, with MG132 treatment added 16 hours before harvesting. nsp16 protein was enriched using Protein-G beads coupled with the nsp16 antibody, and interactions and ubiquitination were analyzed by immunoblotting (IB) with endogenous antibodies against MARCHF7, UBR5, and ubiquitination.
(B-I). MARCHF7 and UBR5 were knocked down by siRNA in Caco2 cells. 24 h after transfection, the cells were infected with Wuhan strain (MOI:0.01) (C-E) or Omicron BA.1 strain (MOI: 0.001) (F-H), respectively. 2 h post infection, the supernatant was discarded, and the cells were cultured in DMEM containing 3% fetal bovine serum for 48 h. The mRNA levels of SARS-CoV-2 *M* and *E* genes in the cells (C, F) and *E* genes in supernatant (D, G) were detected by RT-qPCR and the viral titers in supernatant (E, H) were measured. The N protein levels of Wuhan or Omicron viruses were detected by IB (I). Knock-down efficiencies of MARCHF7 and UBR5 were detected by RT-qPCR or IB (B, I). Data are representative of three independent experiments and shown as average ±SD (n = 3). Significance was determined by one-way ANOVA, followed by a Tukey multiple comparisons posttest: *P < 0.05; **P < 0.01; ***P < 0.001.

significantly increased intracellular and secreted viral mRNA levels (*M* and *E* genes) of both strains. Additionally, with the Wuhan strain, MARCH7 knockdown resulted in a 0.6-log increase in viral titre in the supernatants, while UBR5 knockdown caused an over 1-log increase. With the Omicron strain, knockdown of the two E3 ligases resulted in an even greater increase in viral titres (**Fig. 5C–E** for the Wuhan strain and 5F–H for the Omicron strain). Immunoblotting (IB) confirmed these findings, demonstrating elevated intracellular and secreted N protein levels upon UBR5 or MARCH7 knockdown (**Fig. 5I**). The knockdown efficiency of MARCHF7 and UBR5 was also confirmed (**Fig. 5B**). Due to low transfection efficiency in Caco2 cells, we overexpressed UBR5-Myc or MARCH7-Myc in HEK293T-ACE2 cells. Overexpression of UBR5 or MARCH7 significantly decreased viral mRNA levels of the *M* and *E* genes in both the Wuhan and Omicron strains, as measured by real-time quantitative polymerase chain reaction (RT-qPCR). IB analysis also showed decreased N protein levels in cells and supernatants, accompanied by a decrease in viral titres of more than 0.5-log. However, co-transfection with increasing amounts of nsp16 significantly abrogated the inhibitory effects of UBR5 and MARCH7 on SARS-CoV-2 replication (**Fig. 6A–H** and **Figure 6—figure supplement 1A–H**). To eliminate the potential influence of nsp16's intrinsic function on experimental outcomes, we overexpressed UBR5 with an inactive HECT domain (UBR5-ΔHECT) or MARCHF7 with a RING domain deletion (MARCHF7-1-542), along with nsp16. These E3 ligase mutants failed to inhibit viral replication. Moreover, a gradual enhancement of nsp16 protein expression did not enhance viral replication. While there was a slight increase in the mRNA levels of *M*, protein levels of E and N remained unchanged (**Figure 6 — figure supplement 2A–H**). These results suggest that UBR5 and MARCH7 exhibit antiviral activity against SAR-CoV-2 of UBR5 and MARCHF7 through their enzymatic function, significantly suppressing viral replication by targeting nsp16 for degradation.

UBR5 and MARCHF7 mediate broad-spectrum degradation of nsp16 variants

Given the ongoing emergence of SARS-CoV-2 variants, broad-spectrum antiviral activity remains critical. To investigate whether UBR5 and MARCH7 can mediate broad-spectrum degradation of various nsp16 variants, we aligned the amino acid sequences of nsp16 proteins obtained from the National Center for Biotechnology Information (**Figure 6 — figure supplement 3A**). Among these, only three variants, XBB.1.9.1, XBB.1.5, and XBB.1.16, exhibited a higher number of mutation sites compared to other variants, which showed only one or two mutations, suggesting a more conserved sequence. Consequently, using mutagenesis techniques, we synthesised the nsp16 sequences for these three variants along with several single-site mutants from other variants. Treatment with the proteasome inhibitor MG132 restored nsp16 protein levels for all variants (**Figure 6—figure supplement 3B**), confirming that degradation occurs through the UPS. Furthermore, knockdown of either UBR5 or MARCHF7 increased the stability of nsp16 proteins from these variants, albeit to varying degrees, indicating that these nsp16 proteins are sensitive to UBR5- or MARCHF7-mediated degradation (**Figure 6 — figure supplement 3C**). Taken together, these findings suggest that UBR5 and MARCHF7 may confer broad-spectrum antiviral activity by targeting nsp16 from diverse SARS-CoV-2 for degradation.

SARS-CoV-2 infection reduces UBR5 and MARCHF7 expression

To explore the relationship between SARS-CoV-2 infection and the expression levels of UBR5 and MARCHF7, we analysed changes in their mRNA and protein levels after infection with either the Wuhan or Omicron strains at varying MOIs, using RT-qPCR and IB, respectively. Both mRNA and protein levels of MARCFH7 decreased with increasing viral titres. However, UBR5 expression initially increased at low titres but continuously declined with increasing titres (**Figure 6 — figure supplement 4A-4C**). Previous studies have reported a role for UBR5 in regulating interferon-γ-mediated pathways, which might explain the observed increase in UBR5 expression at low titres (Wu et al., 2022). To confirm these findings *in vivo*, we examined UBR5 and MARCHF7 mRNA levels in peripheral blood mononuclear cells from SARS-CoV-2-infected patients with varying

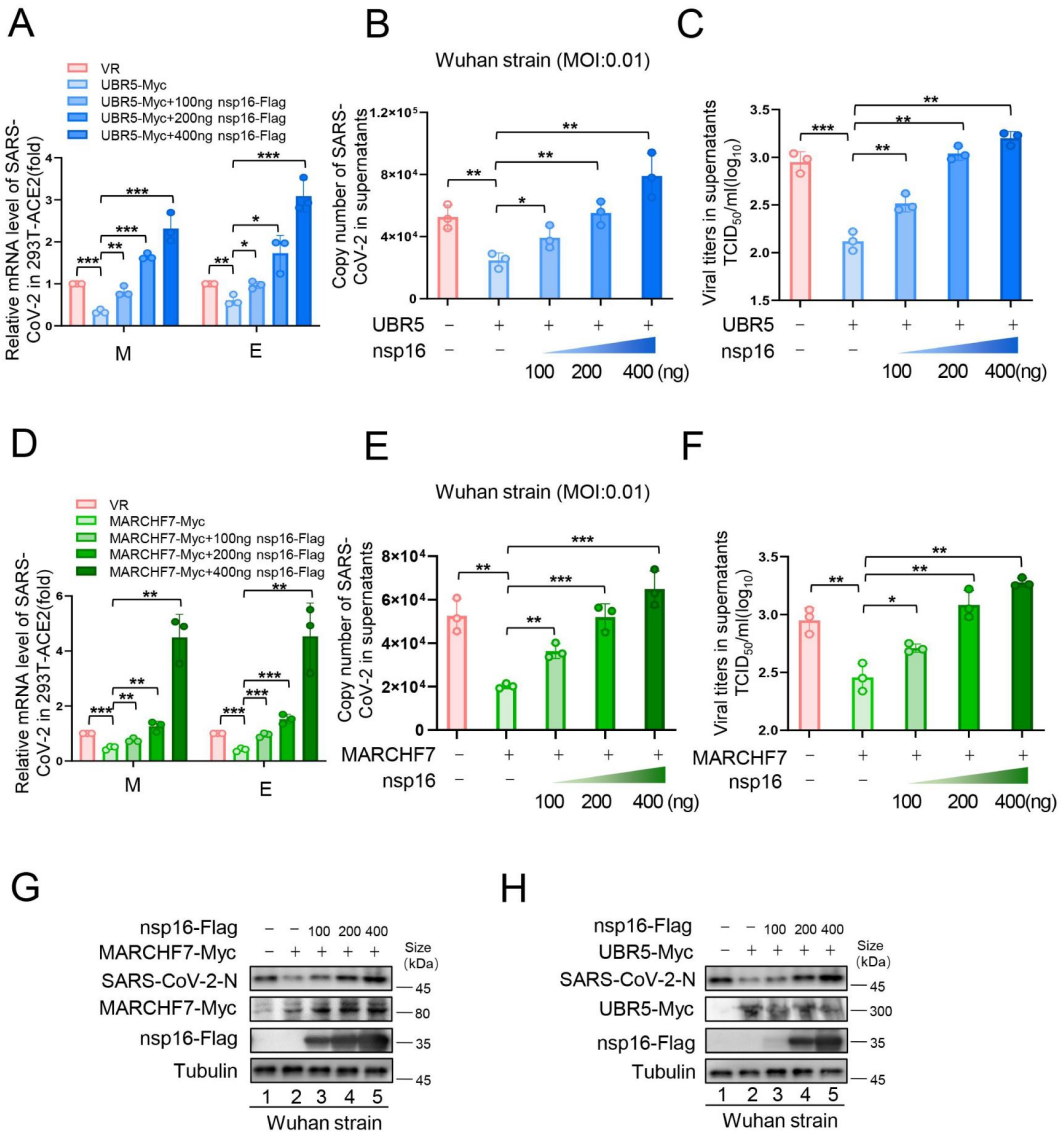

Figure 6.

Increased levels of nsp16 rescued viral inhibition by UBR5 or MARCHF7'

(A-H) UBR5 or MARCHF7 was transfected in 293T cells stably overexpressed with ACE2, and the increased doses of nsp16-Flag was transfected simultaneously. After 24 h, the cells were infected with Wuhan strains. The mRNA levels of *M* and *E* genes of Wuhan strain in the cells (A, D) and *E* gene in supernatant (B, E) were detected by RT-qPCR, as well as the detection of viral titers in supernatant (C, F). The N protein of the virus and the overexpression efficiency was detected by IB (G, H). Data are representative of three independent experiments and shown as average ±SD (n = 3). Significance was determined by one-way ANOVA, followed by a Tukey multiple comparisons posttest. P > 0.05; **P < 0.01; ***P < 0.001. **Figure 6 — figure supplement 1** shows data related to infection with Omicron BA.1.

disease severity. While UBR5 mRNA levels negatively correlated with disease progression, MARCHF7 levels showed no significant correlation (**Figure 6 — figure supplement 4D**). These results suggest that SARS-CoV-2 may suppress host antiviral defences mediated by UBR5 and MARCHF7.

UBR5 and MARCHF7 protect mice from SARS-CoV-2 challenge

Given the lack of known activators or inhibitors for E3 ligases, we developed a transient overexpression method for UBR5 and MARCH7 in mice using high-pressure tail vein injection of plasmids (Bonamassa et al., 2011). To assess their *in vivo* antiviral effects, mice were injected with plasmids encoding UBR5 or MARCH7, followed by SARS-CoV-2 challenge (**Fig. 7A**). Both MARCHF7 and UBR5 overexpression significantly decreased viral *E* gene copy numbers in mouse lungs compared to those in the control group, as well as markedly decreased viral titres in lung tissue homogenates (**Fig. 7C-D**). Additionally, treated mice experienced less weight loss (**Fig. 7E**). Histopathological analysis of major organs 5 d post-infection revealed that lungs from mice treated with UBR5 or MARCH7 displayed attenuated lesions, including alveolar contraction and pulmonary oedema, compared to those typically observed in control mice (**Fig. 7F**). These treatments also reduced the abundance of N proteins (**Fig. 7G**). Collectively, these results suggest that UBR5 or MARCH7 overexpression inhibits SARS-CoV-2 virulence *in vivo* by promoting nsp16 protein degradation.

SARS-CoV-2 infection can trigger a severe cytokine storm, thought to be responsible for its high mortality rates (Song et al., 2020) (Hojyo et al., 2020). To examine the effect of UBR5 and MARCH7 on inflammatory responses, we measured levels of key cytokines, including interleukin-6, interleukin-1 receptor antagonist, and interleukin-1β, in the spleens of SARS-CoV-2-infected mice (Makaremi et al., 2022) (Hu et al., 2021). Consistent with their antiviral activity, treatment with UBR5 or MARCH7 significantly reduced the production of these cytokines (**Fig. 7H**).

Discussion

SARS-CoV-2 nsp16 functions as a 2'O-MTase, catalysing the methylation of the penultimate nucleotide of the viral RNA cap. This modification produces a 5'-RNA cap structure that mimics host RNA, thereby evading host immune detection and responses (Lin et al., 2020) (Balieiro et al., 2022; Russ et al., 2022). High-resolution structures of nsp16 and nsp16-nsp10 heterodimers have been characterised (Rosas-Lemus et al., 2020) (Klima et al., 2022; Lugari et al., 2010), paving the way for antiviral drug development targeting these heterodimers (Balieiro et al., 2022; Melo-Filho et al., 2022). However, the host factors that interact with and regulate nsp16 remain largely unknown.

Previously, our group and others have demonstrated the importance of the UPS in modulating SARS-CoV-2 infection (Xu et al., 2022). For example, host E3 ligases, such as RNF5, Cullin4-DDB1-PRPF19, ZNF598, and TRIM7, ubiquitinate and degrade key SARS-CoV-2 proteins, thereby suppressing viral replication (Li et al., 2023; Liang et al., 2022; Maimaitiyiming et al., 2022; Zhang et al., 2024). Conversely, SARS-CoV-2 employs DUBs to counteract these host defences and enhance its replication (Chen et al., 2024; Gao et al., 2024; Gao et al., 2022; Guo et al., 2021). In this study, we identify nsp16 as a short-lived protein with a half-life of only 2–3 h that is targeted for ubiquitination and degradation by the UPS. Using MS and bioinformatics screening, we identified two E3 ligases, UBR5 and MARCHF7, that directly interact with and target nsp16 for ubiquitination and degradation.

UBR5 is a member of the UBR box protein family and contains a HECT domain essential for its E3 ligase activity (Kim et al., 2021). It is known to regulate tumour growth, metastasis (Xiang et al., 2022) (Qiao et al., 2020), and viral infections. For example, URB5 targets Middle East

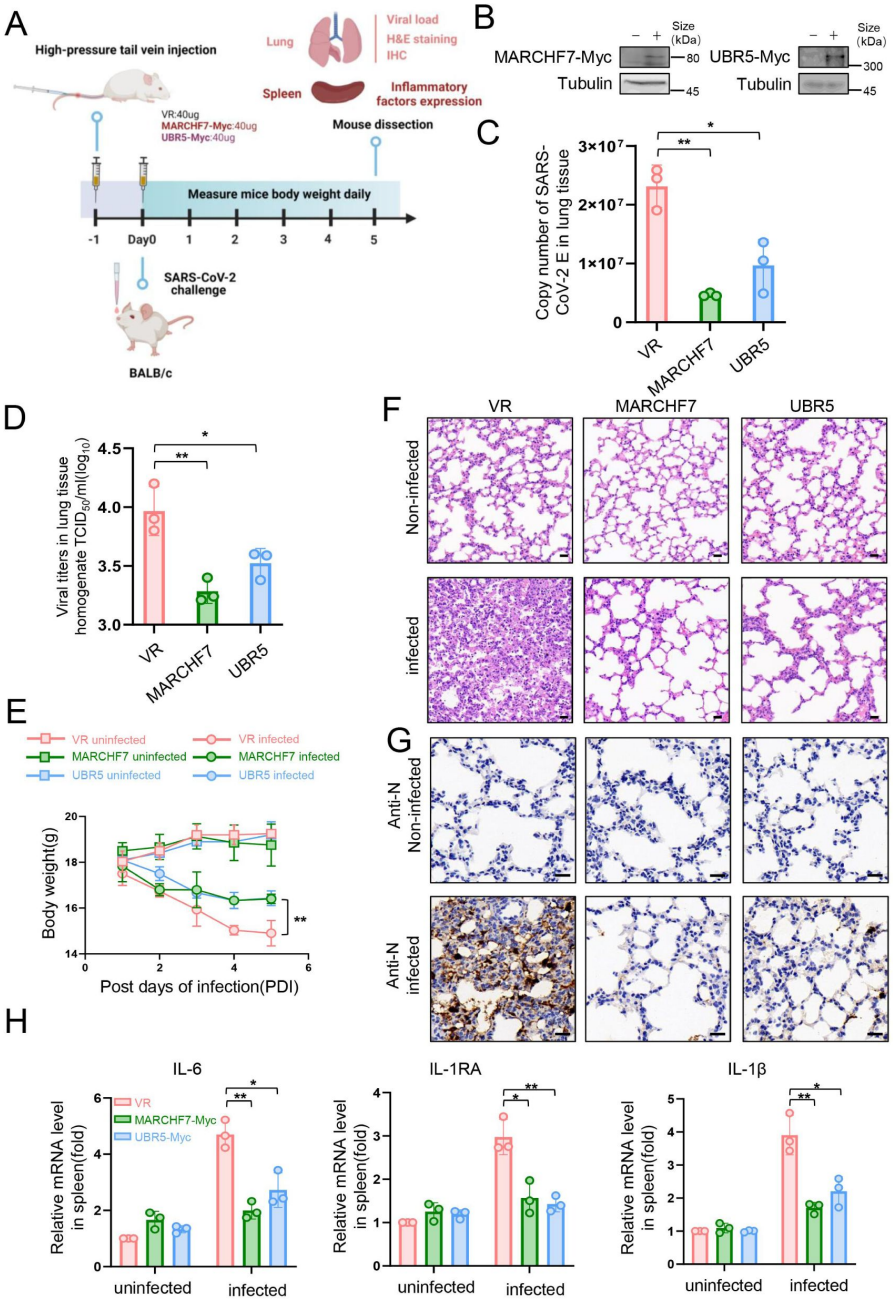

Figure 7.

In a mouse infection model, overexpression of MARCHF7 or UBR5 exerted inhibitory effects on virus.

(A-G) BLAB/C mice were injected with the corresponding plasmids at 40ug/500ul via the high-pressure tail vein, followed by nasal inoculation with 50μl SARS-CoV-2 virus at a dosage of $10^{5.5}$ TCID50/mL (created using *BioRender.com*). IB was used to detect the expression of MARCHF7 or UBR5 in the lung tissues (B). Viral RNA loads in mouse lung tissues were detected by measuring the mRNA levels of the E genes by RT-qPCR (C). Lung tissue was collected, homogenized, and the residue was removed by centrifugation to collect the supernatant. The viral titer was then measured using the TCID50 method (D). Mouse body weight was monitored during the experimental period (E). Representative images of H&E staining of lungs of mice with different treatments. Magnification, ×40. Bars, 20 μm (F). The staining of viral N proteins. Magnification, ×63. Bars, 20 μm. n =3 in each group (G). RT-qPCR was used to measure the expression of cytokines and chemokines in the spleens of mice in each group (H). Statistical significance was analyzed using a one-way analysis of variance with Tukey's multiple comparisons test. (NS, no significance, *p < 0.05, **p < 0.01, ***p < 0.001).

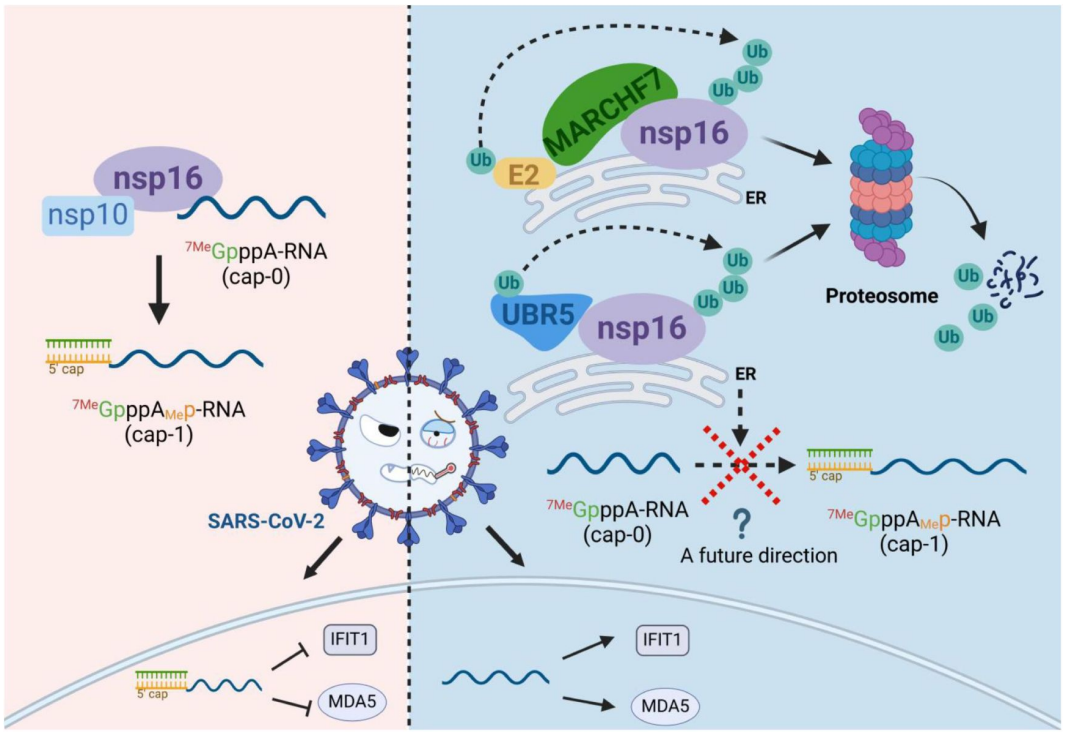

Figure 8.

Schematic diagram of MARCHF7 and UBR5 ubiquitinate the SARS-CoV-2 non-structural protein nsp16, leading to its degradation via the proteasomal pathway, thereby affecting viral replication (created using *BioRender.com*).

respiratory syndrome coronavirus ORF4b protein for degradation, dampening the host immune response (Zhou et al., 2022). Conversely, UBR5 acts as a cofactor for Zika virus replication by helping TER94/VCP degrade the capsid protein to expose the viral genome to the cytoplasm (Gestuveo et al.). MARCHF7 is a RING E3 Ub ligase that regulates T cell proliferation, neuronal development, inflammasomes, and tumour progression (Zheng, 2021) (Zhang et al., 2016) (Cai et al., 2022) (Zhao et al., 2018). However, its role in viral infections has been largely unexplored, with only one study identifying it as a host protein interacting with the 2C of foot-and-mouth disease virus (Mahajan et al., 2021).

Our findings reveal that UBR5 and MARCHF7 independently interact with nsp16 and facilitate its degradation, primarily within the cytoplasmic side of the ER. This reflects an evolutionary arms race between viruses, which develop mechanisms to resist host antiviral responses, and hosts, which deploy multiple strategies to counteract the virus. One such strategy is seen with multiple E3 ligases that target the same viral protein for degradation. Functional analyses demonstrate that UBR5 or MARCHF7 knockdown enhanced SARS-CoV-2 replication, whereas their overexpression impaired replication. Furthermore, we found that when the enzymatic activity of these E3 ligases is inactivated, their antiviral effect is abolished, indicating that their antiviral effects are dependent on their E3 ligase activity. Additionally, we observed that in the absence of functional UBR5 or MARCH7, overexpression of nsp16 does not increase viral levels. This suggests that although nsp16 plays an important role, it cannot independently promote viral replication without the involvement of E3 ligases. This underscores the critical function of UBR5 and MARCHF7 as antiviral factors that suppress SARS-CoV-2 replication by promoting nsp16 degradation.

Notably, while nsp16 possesses 18 lysine residues, identifying specific ubiquitination sites proved challenging. Based on structural data of nsp16 (Decroly et al., 2011), we constructed truncated nsp16 mutants to assess their degradation profiles. We found that nsp16 could still be degraded to varying degrees (Appendix-figure S2A-B), suggesting that multiple lysine residues serve as recognition sites for E3 ligases. Nonetheless, the results from these truncated mutants regarding the MG132 recovery provided us with valuable insights. For instance, the Δ2-17 mutant, which lacks this segment, showed more than a two-fold increase in nsp16 expression levels. Conversely, the Δ204-212 mutant exhibited significantly reduced recovery after MG132 treatment compared to the wild-type. These observations offer important clues for further investigation into the interaction regions between nsp16 and MARCHF7 or UBR5, as well as potential ubiquitination sites. MS analysis identified K76 of nsp16 as a ubiquitination site (Appendix-figure S2C). However, an nsp16 K76R mutant was still degraded by E3 ligases, although the degree of ubiquitination was reduced compared to that of the wild-type, indicating that K76 might be one of several potential ubiquitination sites (Appendix-figure S2D-E). Therefore, we hypothesise that nsp16 undergoes ubiquitination at multiple sites and may involve non-canonical ubiquitination pathways at non-lysine residues (McClellan et al., 2019). A comprehensive understanding of the ubiquitination landscape of nsp16 requires further investigation. In addition to UBR5 and MARCHF7, other E3 ligases could contribute to nsp16 regulation, which warrants further studies.

Currently, no specific activators or inhibitors exist for UBR5 or MARCH7. To validate their antiviral effects *in vivo*, we employed high-pressure tail vein injection, a method commonly used for gene delivery to the liver (Kamimura et al., 2014). This method has also been shown to facilitate gene delivery to other tissues, including the lungs (Bonamassa et al., 2011). Gene expression was successfully detected in lung tissues. While this method induced mild immune activation, its effect is relatively minimal compared with that of other techniques (Suda et al., 2023). Moreover, studies suggest that mice and non-human primates exhibit higher resistance to innate immune activation than humans, suggesting that our findings were only minimally influenced by immune activation (Raper et al., 2003). However, this highlights that translating new drug targets into therapeutic treatments will require considerable time and effort. For example, human trials involving the injection of naked DNA (e.g., OTC cDNA) have shown variable outcomes. While no severe immune responses were observed in most participants, one case of fatal immune activation

was reported (Raper et al., 2003), highlighting the variability of human immune responses and a key limitation in extrapolating findings from animal models to human trials. This variability might also explain why we did not observe a clear trend for MARCHF7 mRNA levels in peripheral blood samples from patients with varying disease severities. The limited number of patients in our study could further contribute to this observation.

In this study, we identified the host E3 ligases, UBR5 and MARCHF7, as critical regulators of SARS-CoV-2 nsp16 through ubiquitination and subsequent degradation. We demonstrated a negative correlation between the expression levels of these ligases and the degree of infection, underscoring their antiviral roles. Furthermore, both ligases significantly inhibit SARS-CoV-2 replication. Our findings pave the way for the development of novel therapeutic strategies targeting the UPS for the treatment of COVID-19.

Materials and Methods

Reagents and antibodies

The drugs used in this study were as follows: MG132 (catalog no. S2619), Bafilomycin A1 (catalog no. S1413), Bortezomib (catalog no. S1013), Carfilzomib (catalog no. S2853) and Vinblastine (catalog no. S4504) were purchased from Selleck (Houston, TX, USA). Cycloheximide (catalog no. 66-81-9) was purchased from Sigma (Saint Louis, MO, USA). The antibodies used for immunoblotting analysis (IB) were as follows: anti-UBR5 mAb (Proteintech, Rosemont, IL, USA, catalog no. 66937-1-Ig), anti-MARCHF7 mAb (Santa Cruz Biotechnology, Dallas, TX, USA, catalog no. sc-166945), SARS-CoV-2 2'-O-ribose Methytransferase Antibody (nsp16) (Cell signaling, Danvers, Massachusetts, USA, catalog no. #70811), anti-Flag mAb (Sigma, catalog no. F1804), anti-tubulin mAb (Abcam, Cambridge, Cambridgeshire, UK, catalog no. ab11323), anti-hemagglutinin (anti-HA) pAb (Invitrogen, catalog no. 71-5500), anti-Myc pAb (Proteintech, Rosemont, IL, USA, catalog no. 16286-1-AP), and anti-GFP mAb (Abcam, catalog no. ab1218). Primary antibody: anti-COX5A pAb (Sangon Biotec, Shanghai, CHN, catalog no. D261450), anti-PDI-mAb (Proteintech, catalog no. 2E6A11) and Human GM130/GOLGA2 Antibody (R&D Systems, Minneapolis, MN, USA, catalog no. AF8199) were used for immunofluorescence, and SARS-CoV-2 nucleocapsid monoclonal antibody (mAb) (GeneTex, Irvine, CA, USA, catalog no. GTX635679) were used for Immunohistochemistry. Fluorescent secondary antibodies: goat anti-Rabbit IgG (H+L) Highly Cross Adsorbed Secondary Antibody, Alexa Fluor Plus 488 (Invitrogen, catalog no. A11001), and goat anti-Rabbit IgG (H+L) Highly Cross Adsorbed Secondary Antibody, Alexa Fluor Plus 568 (catalog no. A-11011) and immunohistochemical secondary antibodies: Streptavidin-Peroxidase Anti-Rabbit IgG kit (catalog no. KIT-9706) were purchased from Invitrogen and maixin (Fuzhou, CHN) respectively.

Cell lines and viruses

The cell lines used in this study include HEK293T cells (catalog no. CRL-11268), Hela cells (catalog no.CRM-CCL-2), Caco2 cells (catalog no. HTB-37). All cell lines were purchased from American Type Culture Collection (ATCC; Manassas, VA, USA) and tested for mycoplasma. In order to conduct virus related experiments, stable cell lines including Caco2-N^{int} (stably expressing SARS-CoV-2 N gene) and 293T-ACE2 (stably expressing ACE2) were generated in our laboratory. The cells were cultured in a cell incubator containing 5% CO2 at 37°C using Dulbecco's modified Eagle's medium (DMEM; HyClone, Logan, UT, USA) containing 10% heat-inactivated fetal calf serum (FCS, GIBCO BRL, Grand Island, NY, USA), 100 mg/ml penicillin, and 100 ug/ml streptomycin to provide nutrition. We expanded SARS-CoV-2 virus-like-particles (Wuhan-Hu-1, MN908947, Clade:19A) with high replication capacity in Caco2-N^{int} using a biosafety level-2 (BSL-2) cell culture system. The virus infecting the cells include Omicron BA. 1 strain (human/CHN_CVRI-01/2022) and SARS-CoV-2 Wuhan strain (BetaCoV/Beijing/IME-BJ05-2020, GenBank access no. MT291831.1), and mouse

adapted SARS-CoV-2/C57MA14 variant (GenBank: OL913104.1) used for experiments in mice were provided by Key Laboratory of Jilin Province for Zoonosis Prevention and Control, and all experiments for virus infection were performed in Biosafety level 3 (BSL-3) cell culture system.

Plasmids

Eukaryotic expression plasmids encoding SARS-CoV-2 nsp protein were provided by Professor Wang Peihui (Shandong University). The nsp16-HA expression vector was constructed by adding HA tag at the C-terminus. UBR5 (Gnen ID: 51366) and its mutants (UBR5-ΔHECT, UBR5-ΔPABC, UBR5-ΔUBR) expression plasmids were constructed using purchased plasmids from Addgene (Watertown, MA, USA) as templates with no tag or a MYC tag at the N-terminus. The cDNA of 293T cells was used as a template to construct MARCHF7(Gene ID: 64844) and its truncated mutant with a Myc tag at the C-terminus. All the above expression plasmids were inserted into the VR1012 vector. For immunofluorescence (IF) and Fluorescence Resonance Energy Transfer (FRET) experiments, pCDNA3.1-YFP vector (catalog no. 13033) and pECFP-C1 vector (catalog no. 6076-1) were purchased from Addgene and BD (Biosciences Clontech), and MARCHF7 or UBR5 was constructed on pECFP-C1, and nsp16 was constructed on pCDNA3.1-YFP. Single point mutants of nsp16 of different virus subtypes were obtained by point mutagenesis. Multi-site combined mutants were synthesized by Sangon Biotec Company. Human ubiquitin protein and its mutants have been previously described. Primers required for PCR were listed in Appendix Table S1.

RNA extraction and real-time quantitative PCR

We used the way of Trizol (Invitrogen, catalog no. 15596018CN) to extract RNA. The RNA was subsequently reverse transcribed using a High-Capacity cDNA Reverse Transcription kit (Applied Biosystems, Carlsbad, CA, USA, catalog no. 4368814). Finally, PrimeScript RT Master Mix (Takara, Shiga, JPN, catalog no. RR036A) and relative real-time primer were used for qPCR on an Mx3005P instrument (Agilent Technologies, Stratagene, La Jolla, CA, USA). Amplification procedure of the target fragment is as follows: predenaturation at 95°C for 2min, denaturation at 95 °C for 30s, annealing at 55 °C for 30s, and extension at 72 °C for 30s, total of 40 cycles. Real-time primer sequences used in this study were shown in appendix table S1.

Immunoblotting analysis (IB)

Cells or supernatant cultured for a certain time were collected, cell precipitates were resuspended with lysis buffer (50 mM Tris–HCl [pH 7.8], 150 mM NaCl, 1.0% NP-40, 5% glycerol and 4 mM EDTA), 4xloading buffer was added (0.08M Tris [pH 6.8], 2.0%SDS, 10% glycerol, 0.1 M dithiothreitol, and 0.2% bromophenol blue), and samples were lysed by heating at 100℃ for 30min. After removal of cell debris by centrifugation, the supernatant was taken to separate proteins of different sizes by SDS-PAGE. The proteins were transferred onto polyvinylidene fluoride (PVDF) membranes, incubated overnight with the indicated primary antibody, and after 1 hour at room temperature with HRP-conjugated secondary antibodies (Jackson Immunoresearch, West Grove, NJ, USA, catalog no. 115-035-062 for anti-mouse and 111-035-045 for anti-rabbit), the proteins were visualized through Ultrasensitive ECL Chemiluminescence Detection Kit (Proteintech, catalog no. B500024).

Stable cell line generation

We purchased the lentiviral vector pLKO.1-puro (catalog no. 8453) from Adggen. ShRNA targeting target genes were designed and synthesized by Sangon Biotech. After annealing, it was inserted into the vector. Lentivirus was generated by transfection with shRNA (cloned in pLKO.1) or control vector, RRE, VSVG and REV, and the cells were screened with 1/1000 puromycin (3 μg/ml, Sigma, catalog no. P8833) after infection 48 hours. The knockdown efficiency was detected by RT-qPCR or IB. The shRNA target sequences used in this study are shown in appendix table S1.

RNAi

Short interfering RNA (siRNA) used in this study were purchased from RiboBio Co. Ltd. (Guangzhou, CHN). The siRNA sequences for knockdown of MARCHF7 or UBR5 are provided in appendix table S1. The siRNA was transfected into the cells by transfection reagent Lipofectamine 2000 (Invitrogen, catalog no. 11668-019), and the corresponding plasmids were transfected 24 hours later using Lipofectamine 3000 Reagent (Invitrogen, Carlsbad, CA, USA, catalog no. L3000-008). The expression of target genes was detected by RT-qPCR or immunoblotting (IB) analysis 48 hours later.

Immunoprecipitation

After 10 hours of MG132 (10 μM) treatment, the cells were harvested, resuspended in 1ml lysis buffer (50 mM Tris-HCl [pH 7.5], 150 mM NaCl, 0.5% NP-40) containing protease inhibitor (Roche, catalog no. 11697498001), placed on the shaker oscillator for 4 hours to lyse, then centrifuged to remove cell debris, and the supernatant was incubated with the antibody and protein G agarose beads (Roche, Basel, Basel-City, CH, catalog no. 11243233001) at 4°C overnight. Protein G agarose beads was washed 6-8 times with wash buffer (20 mM Tris-HCL [pH 7.5], 100 mM NaCl, 0.1 mM EDTA, and 0.05% Tween 20) at 4°C, centrifuged at 800 g for 1 min. The proteins were eluted by adding loading buffer (0.08 M Tris [pH 6.8], 2.0% SDS, 10% glycerol, 0.1 M dithiothreitol, and 0.2% bromophenol blue), the samples were boiled at 100°C for 10min to elate the proteins. The lysates and immunoprecipitations were detected by IB.

Mass spectrometry (MS)

HEK293T were transfected with SARS-CoV-2-nsp16-Flag for 36 hours, and then harvested after 10 hours of treatment with MG132 or DMSO. Proteins were enriched by co-immunoprecipitation assay. And the elutions were analyzed by MS. MS analysis was performed by the national center for protein science (Beijing, CHN).

Immunofluorescence

At 48 hours after transfection, the solution was discarded and cells were washed twice with preheated PBS for 5min each, followed by fixation with 4% paraformaldehyde at 37°C for 10min. After three washes with PBS, permeabilized with 0.2% Triton X-100 for 5 min at 37°C, and then immediately followed by blocking with 10% fetal bovine serum at room temperature for 1 hour. The blocked cells were incubated overnight with the indicated primary antibodies. The next day, after three washes with PBS, the cells were incubated with corresponding secondary antibodies for 1 hour at room temperature in the dark. The nuclei were stained with DAPI (49,6-diamidino-2-phenylindole, Sigma, catalog no. 9542) and then stored in 90% glycerol. The fluorescence was detected by a laser scanning confocal microscope (FV 3000, Olympus, Tokyo, Japan).

Viral infectivity assay

The Caco2 cells were transfected with siRNA by Lipofectamine RNAiMAX Reagent (Invitrogen, catalog no. 13778150) to knockdown UBR5 or MARCHF7 and infected with Wuhan strain (MOI=0.01) or Omicron-BA.1 strain (MOI=0.001) at 24 hours after transfection. After two hours of infection, the Caco2 cells were cultured in fresh medium containing 2% fetal bovine serum for 48 hours. The cells and supernatants were collected.

Viral levels were characterized by RT-qPCR and IB analysis of viral structural proteins. The overexpression plasmid UBR5-Myc, MARCHF7-Myc and nsp16-Flag was transfected in 293T-ACE2 by Lipofectamine 3000 Reagent and infected with virus 24 hours later.

Mouse lines and infections

BALB/C mice, 6 weeks, were purchased from Charles River Laboratories, Beijing. Mice were cultured in groups according to experimental groups. Our study examined male and female animals, and similar findings are reported for both sexes. To reduce animal suffering, all welfare and experimental procedures were carried out in strict accordance with the Guide for the Care and Use of Laboratory Animals and relevant ethical regulations during the experiment. The mice were randomly divided into 6 groups and injected with 40 μg/500 μl MARCHF7 or UBR5 plasmids via the tail vein at high pressure. Three groups of mice were infected 50ul with SARS-CoV-2 isolates by nasal challenge at a dose of $10^{5.5}$ $TCID_{50}$/mL, three groups were not infected with virus as control, and the empty vector injection group was also used as control.

Immunohistochemical analysis

Three mice in each group, a total of 18 mice, were sacrificed after anesthesia. The lungs of mice were collected and fixed in 4% paraformaldehyde fixative. After 2 days, the lungs were progressively dehydrated through different concentrations of ethanol solution, transparently treated, soaked in xylene, and finally embedded in paraffin. Some thin sections obtained through a microtome for hematoxylin and eosin (H&E) staining. The other fraction was incubated with 3% hydrogen peroxide for 5-10 min at room temperature to eliminate endogenous peroxidase activity. SARS-CoV-2 nucleocapsid monoclonal antibody (mAb) (GeneTex, catalog no. GTX635679) and a Streptavidin-Peroxidase Anti-Rabbit IgG kit (Maixin, Fuzhou, CHN, catalog no. KIT-9706) was used to quantify the viral level in lung tissue.

Statistical analysis

The statistical analyses used in the figures have been described in detail in the figure legends. All data were expressed as mean ± standard deviations (SDs). Statistical comparisons were performed using student's t-test, one-way ANOVA, or repeated measurement ANOVA. The differences were statistically significant as follows: *P < 0.05, **P < 0.01, ***P < 0.001; ns is for no meaning

Ethics statement

Collection of inpatient blood was approved by the Ethics Committee of the First Hospital of Jilin University (21K105-001) in accordance with the guidelines and principles of WMA Declaration of Helsinki and the Department of Health and Human Services Belmont Report. All study participants signed an informed consent form. PBMCS were obtained from 9 COVID-19 patients with mild disease, 6 patients with severe disease, and 5 patients with critical disease (Appendix table S2). All animal experiments were approved by the ethics committee of Research Unit of Key Technologies for Prevention and Control of Virus Zoonoses, Chinese Academy of Medical Sciences, Changchun Veterinary Research Institute, Chineses Academy of Agricultural Sciences (IACUC of AMMS-11-2020-006).

Data availability

The authors declare that [the/all other] data supporting the findings of this study are available within the paper [and its supplementary information files]. The mass spectrometry proteomics data have been deposited to the ProteomeXchange Consortium (*http://proteomecentral.proteomexchange.org*) via the iProX partner repository with the dataset identified PXD053961.

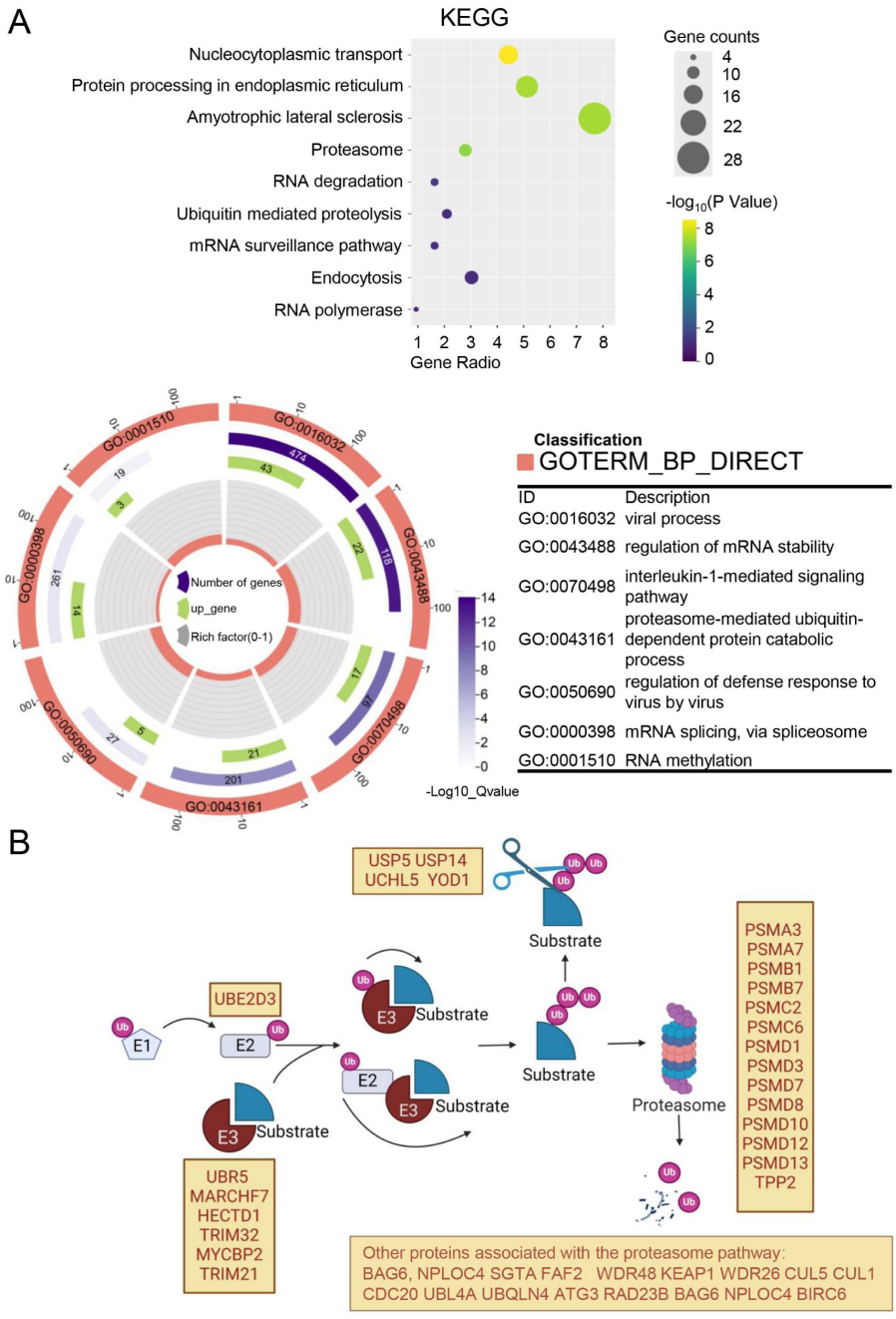

Figure 1—figure supplement 1.

Analysis of mass spectrometry results.

A. The DAVID bioinformatics website (*https://david.ncifcrf.gov/tools.jsp*) was used for KEGG pathway analysis and GO analysis of the differential proteins bound by nsp16 protein after treating with or without MG132. The bubble plots or circle diagram depict the results of the analysis separately. In bubble plots, a change from yellow to purple indicates a decreased p-value, while the size of the circles indicates the number of enriched genes. In the circle plot, depicting the BP (Biological process) analysis in the GO term, the length of the purple rectangle indicates the number of genes included in the term. The length of the green rectangle indicates the number of overlapping genes between the genes included in the term and the genes entered in the gene enrichment analysis, a change from deep to shallow of purple indicates a decreased p-value (created with chiplot.com).

B. Schematic representation of proteins degraded by the proteasome pathway, as well as proteins associated with the proteasome in the MS enrichment analysis are shown (created using *BioRender.com*).

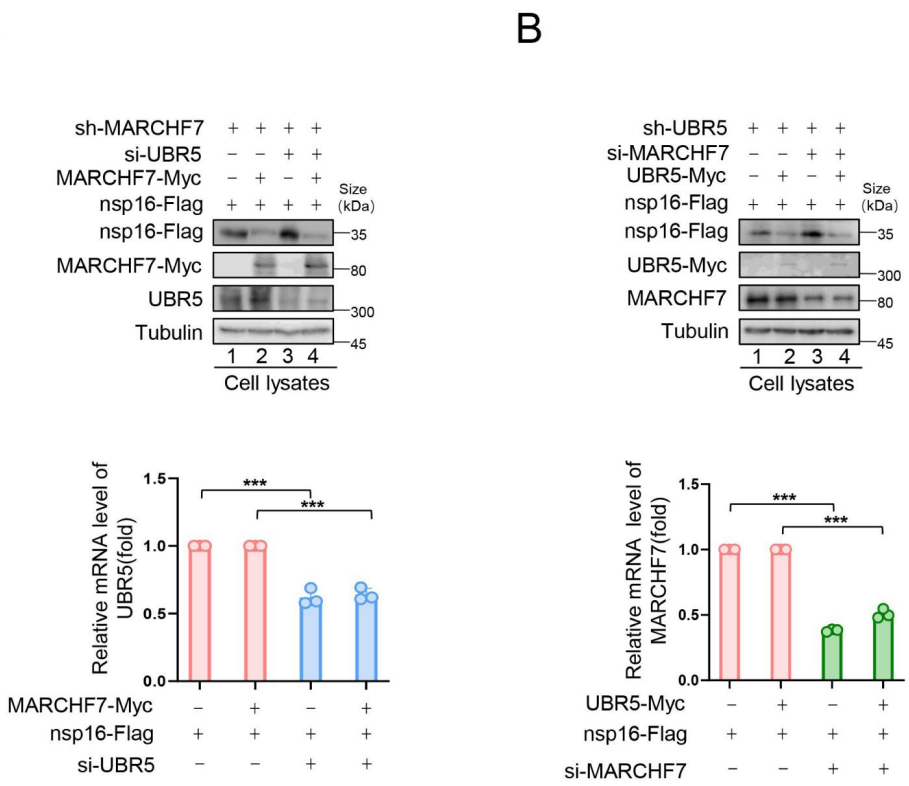

Figure 2—figure supplement 1.

MARCHF7 and UBR5 degrade nsp16 independently.

(A-B). UBR5 siRNA was transfected into shMARCHF7 cells to knock down UBR5. After 24 hours, MARCHF7 and nsp16 expression vectors were co-transfected, and the cells were harvested 72 hours later. The levels of nsp16 were characterized by IB with anti-Flag antibody. Whether MARCHF7 was dependent on UBR5 to degrade of nsp16 was determined by further transfection of MARCHF7 siRNA into shUBR5 cells, followed by co-transfection of UBR5 and nsp16 expression vectors 24 h later. The other operations are the same as above. Data are representative of three independent experiments and shown as average ±SD (n = 3). Significance was determined by a two-tailed t-test. *P > 0.05; **P < 0.01; ***P < 0.001.

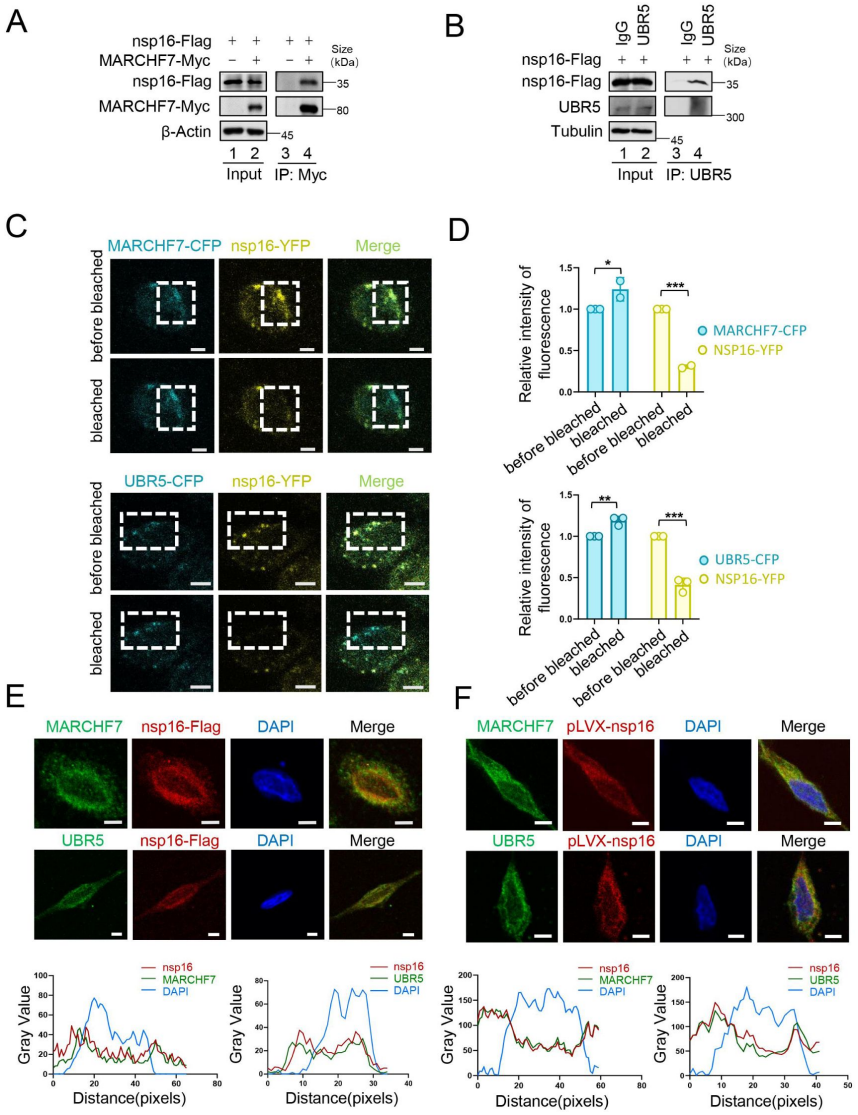

Figure 4—figure supplement 1.

Interaction of MARCHF7 or UBR5 with nsp16.

A. HEK293T cells were transfected with either nsp16-Flag alone or together with MARCHF7-Myc. Thirty-six hours after transfection, the cells were treated with MG132 (10 μM) for 12 h. Cell lysates were subjected to immunoprecipitation with anti-Flag antibody. Using IB to analyze the precipitates and input.

B. HEK293T cells were transfected with nsp16-Flag. Cell lysates were subjected to immunoprecipitation with anti-UBR5 or IgG antibody.

(C-D). Hela cells were co-transfected with YFP-nsp16 and CFP-UBR5 or CFP-MARCHF7. A representative image of YFP-nsp16 (yellow) and ECFP-MARCHF7 (cyan) or ECFP-UBR5 (cyan) expressing cells before and after photobleaching the acceptor fluorophore, YFP. The region chosen for photobleaching is marked (white open box), Bars, 10um. The quantization of fluorescence brightness was analyzed by Image J. Data are representative of three independent experiments and shown as average ±SD (n = 3). Significance was determined by a two-tailed t-test. *P > 0.05; **P < 0.01; ***P < 0.001.

E. HeLa cells transfected with nsp16-Flag were analyzed by confocal microscopy. The Flag-tagged nsp16 labeled with anti-Flag antibody (red). MARCHF7 or UBR5 were labeled with endogenous antibodies (green). Cell nuclei were stained using DAPI (blue). Representative images were shown. Scale bars, 20 um. The ratio of colocalization was quantified by measuring the fluorescence intensities using Image J.

F. nsp16 was stably transfected into HEK293T cells. The cells were analyzed by confocal microscopy. The other operations are the same as above.

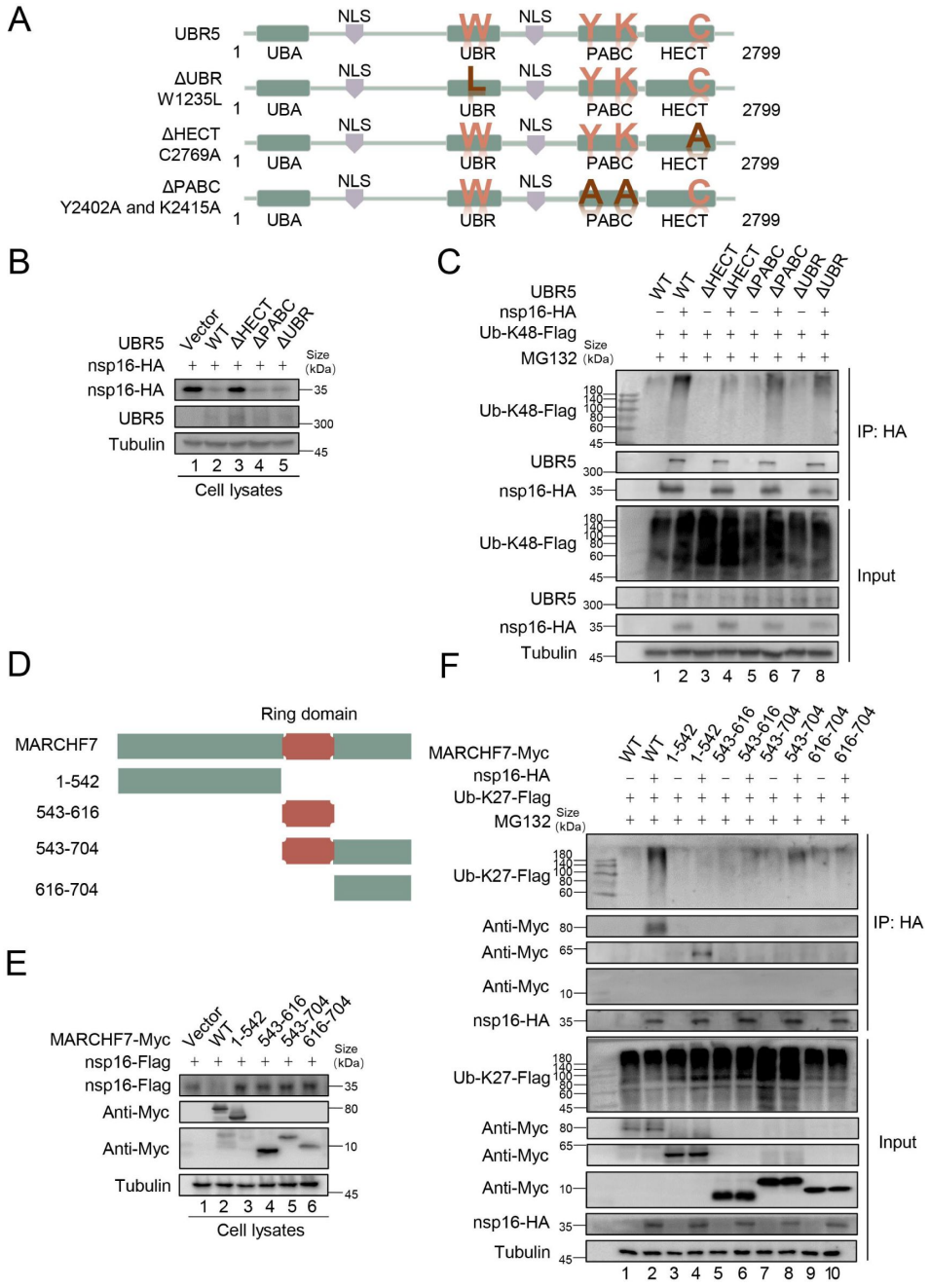

Figure 4—figure supplement 2.

Domains in which MARCHF7 or UBR5 functions.

A. The schematic represents UBR5 WT or mutants used in the study.
B. The HECT domain of UBR5 is required for nsp16 degradation. After co-transfection with UBR5 WT or mutants and nsp16-HA, cells were harvested 48 hours later, and cell lysates were examined by IB.
C. The HECT domain of UBR5 affects K48-type ubiquitin chain of nsp16.HEK293T cells were transfected with the assigned plasmids. After 36 hours, cells were treated with 10 μM MG132 for 12 hours, harvested, and cell lysates were incubated with protein G agarose beads conjugated with anti-HA antibodies. Cell lysates and precipitated samples were analyzed by IB.
D. The schematic represents wild-type and truncated forms of MARCHF7 used in the study. E. Only MARCHF7 wild-type degraded nsp16.
F. The N-terminal region of MARCHF7 interacted with nsp16, and only the wild type could catalyze the K27-type ubiquitin chain of nsp16.

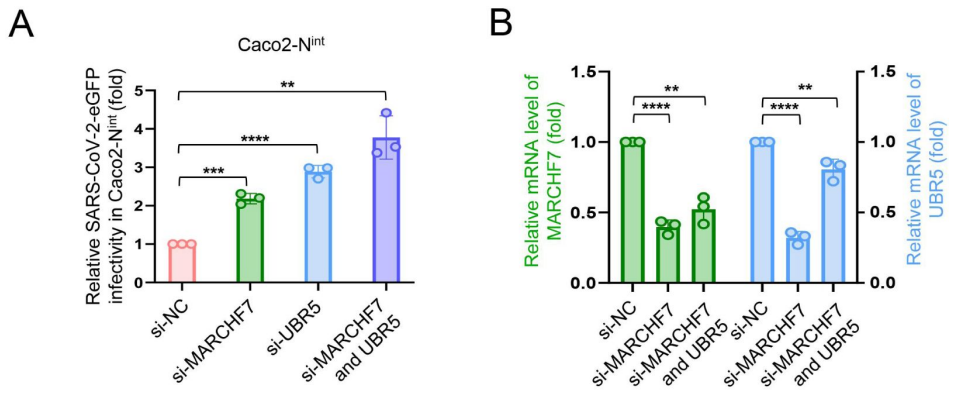

Figure 5—figure supplement 1.

Effect of MARCHF7 or UBR5 on SARS-CoV-2 trVLP.

(A-B). Knocking down MARCHF7 or UBR5 enhances SARS-CoV-2 trVLP infectivity. MARCHF7 or UBR5 was knocked down by siRNA in Caco2 cells with stable expression of SARS-CoV-2 N protein. Twenty-four hours later, cells were infected with SARS-CoV-2 virus-like-particles (MOI:0.1), the medium was changed two hours after infection, and the eGFP-positive cells were detected by flow cytometry 48 hours later (A). Protein content was determined by RT-qPCR (B).

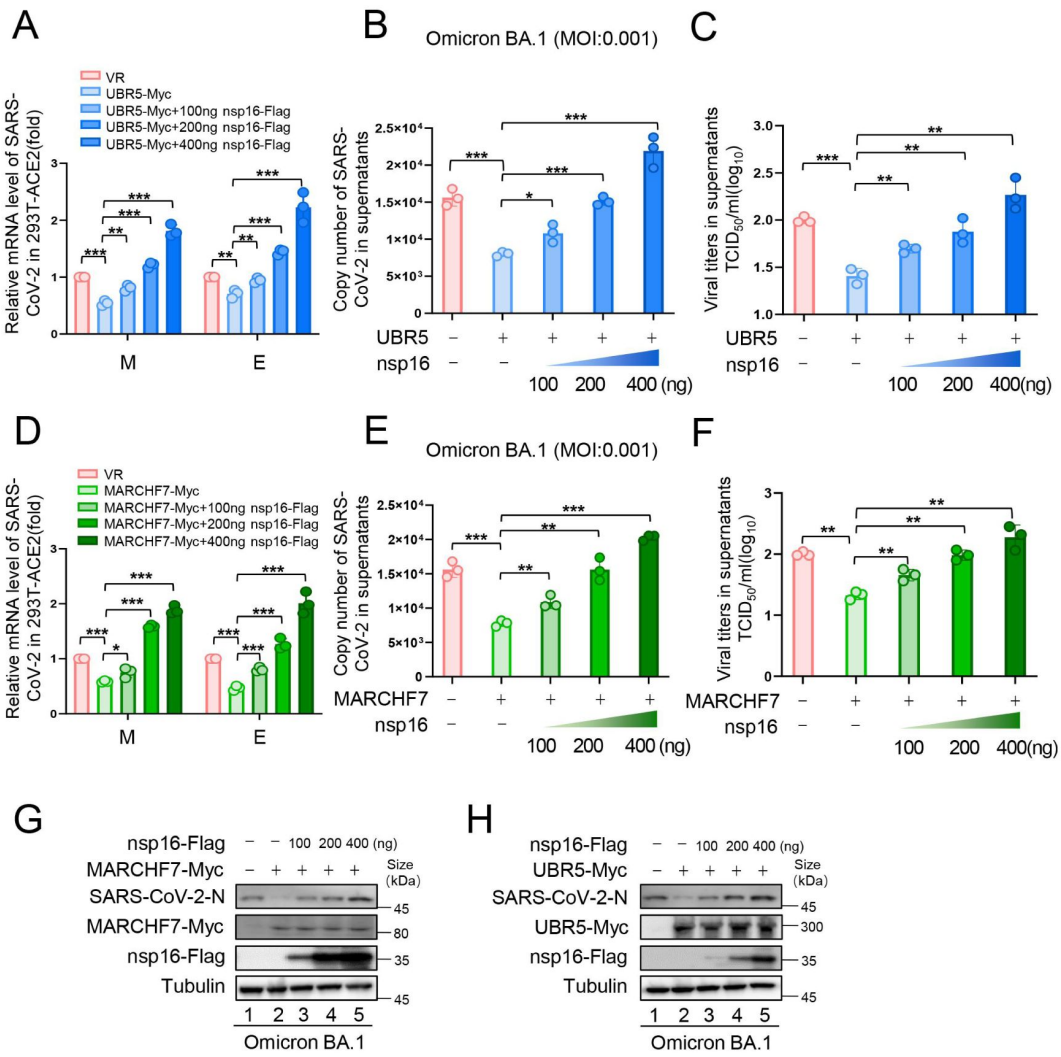

Figure 6 — figure supplement 1.

Effect of MARCHF7 or UBR5 on Omicron BA.1 infectivity.

(A-H). Showing data related to infection with Omicron BA.1. The experimental procedure was the same as **Figure 6**. Data are representative of three independent experiments and shown as average ± SD (n = 3). Significance was determined by one-way ANOVA, followed by a Tukey multiple comparisons posttest. P > 0.05; **P < 0.01; ***P < 0.001.

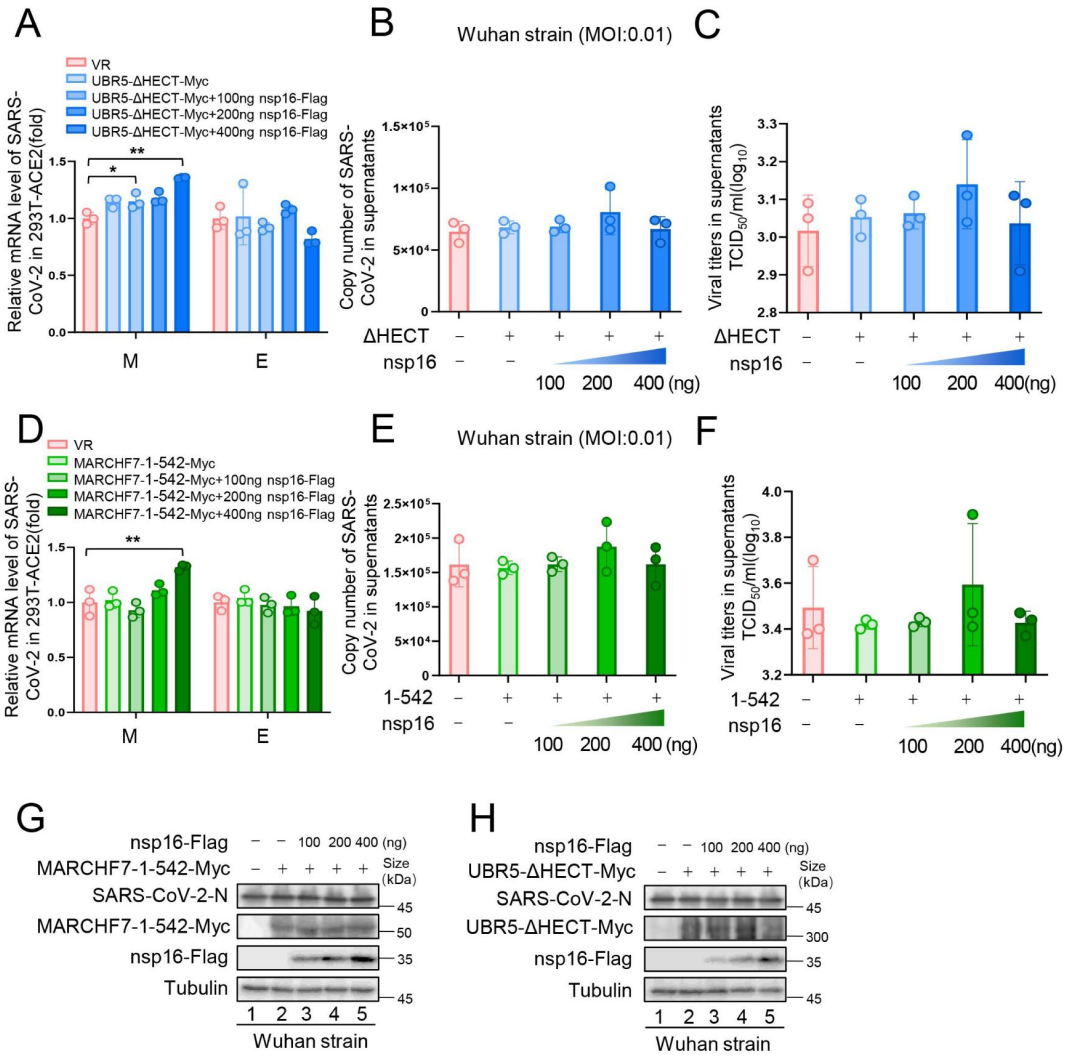

Figure 6—figure supplement 2.

The enzyme activity-deficient mutants do not exhibit antiviral activity, and overexpression of nsp16 does not promote viral replication.

(A-H) In 293T-ACE2 cells, the RING domain deletion mutant of MARCHF7 (MARCHF7-1-542) or the HECT domain inactivated mutant of UBR5 (UBR5- Δ HECT) were transfected, along with a gradient of nsp16-Flag overexpression. The cells were infected with the Wuhan strain (MOI: 0.01), medium was changed 2 hours post-infection, and cells and supernatants were collected 48 hours after infection.

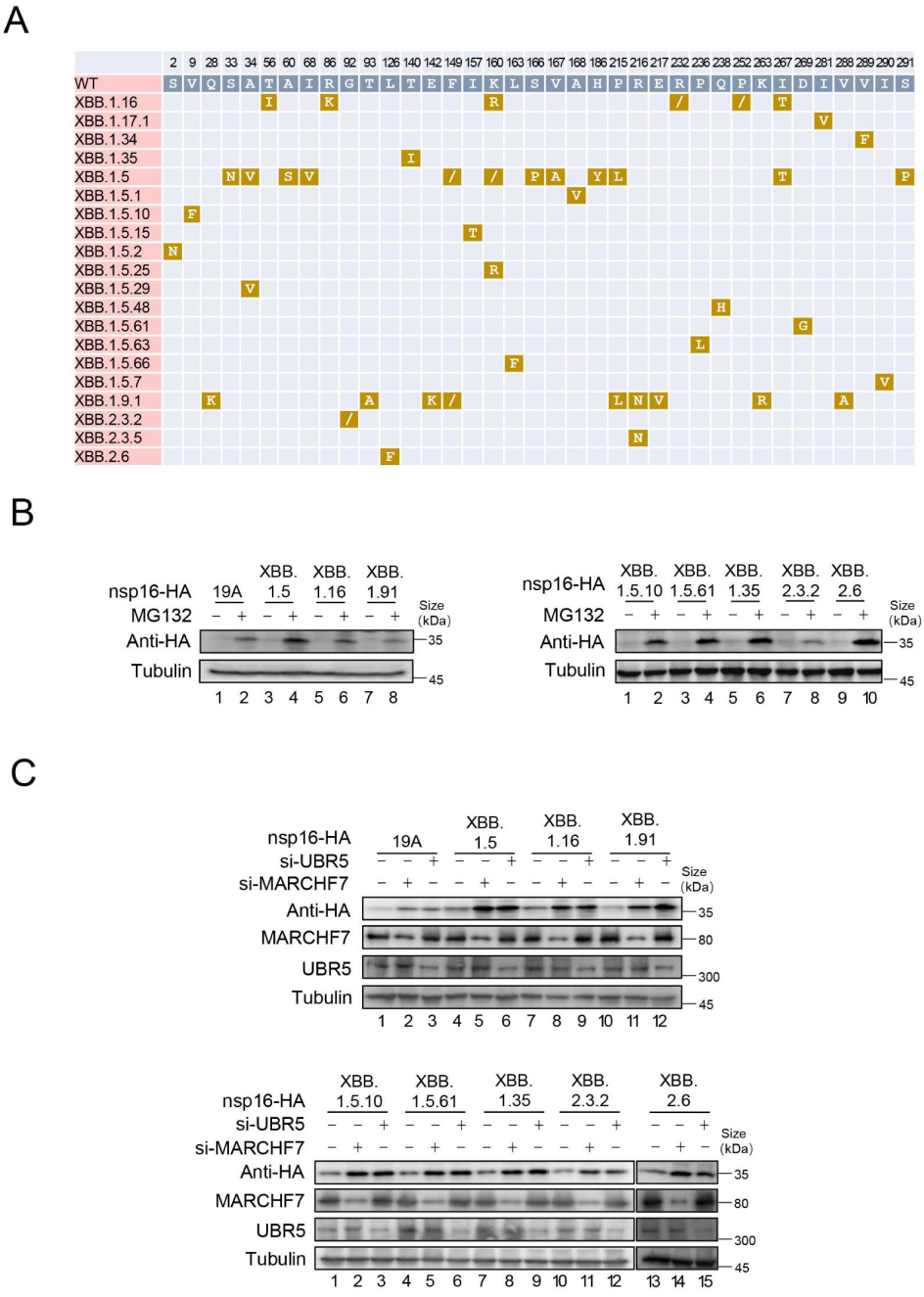

Figure 6—figure supplement 3.

MARCHF7 or UBR5 have effects on mutant of nsp16 in different subtypes of SARS-CoV-2.

A. This diagram shows the mutation of nsp16 in different virus subtypes. The amino acids sequences of different SARS-CoV-2 strains were obtained from NCBI, and the amino acids sequences of nsp16 of different strains were compared by DNAMAN software. B. Nsp16 mutants can still be regulated by MG132. The mutated nsp16 plasmids were transfected into HEK293T cells. After 36 hours of culture, cells were treated with 10 μm MG132 or DMSO, harvested 12 hours late6r, and cell lysates were examined by IB. C. MARCHF7 or UBR5 can degrade nsp16 mutants. After transfecting MARCHF7 or UBR5 siRNA and the mutated nsp16 plasmids, the cells were harvested 48 h later. The cell lysates were detected by IB.

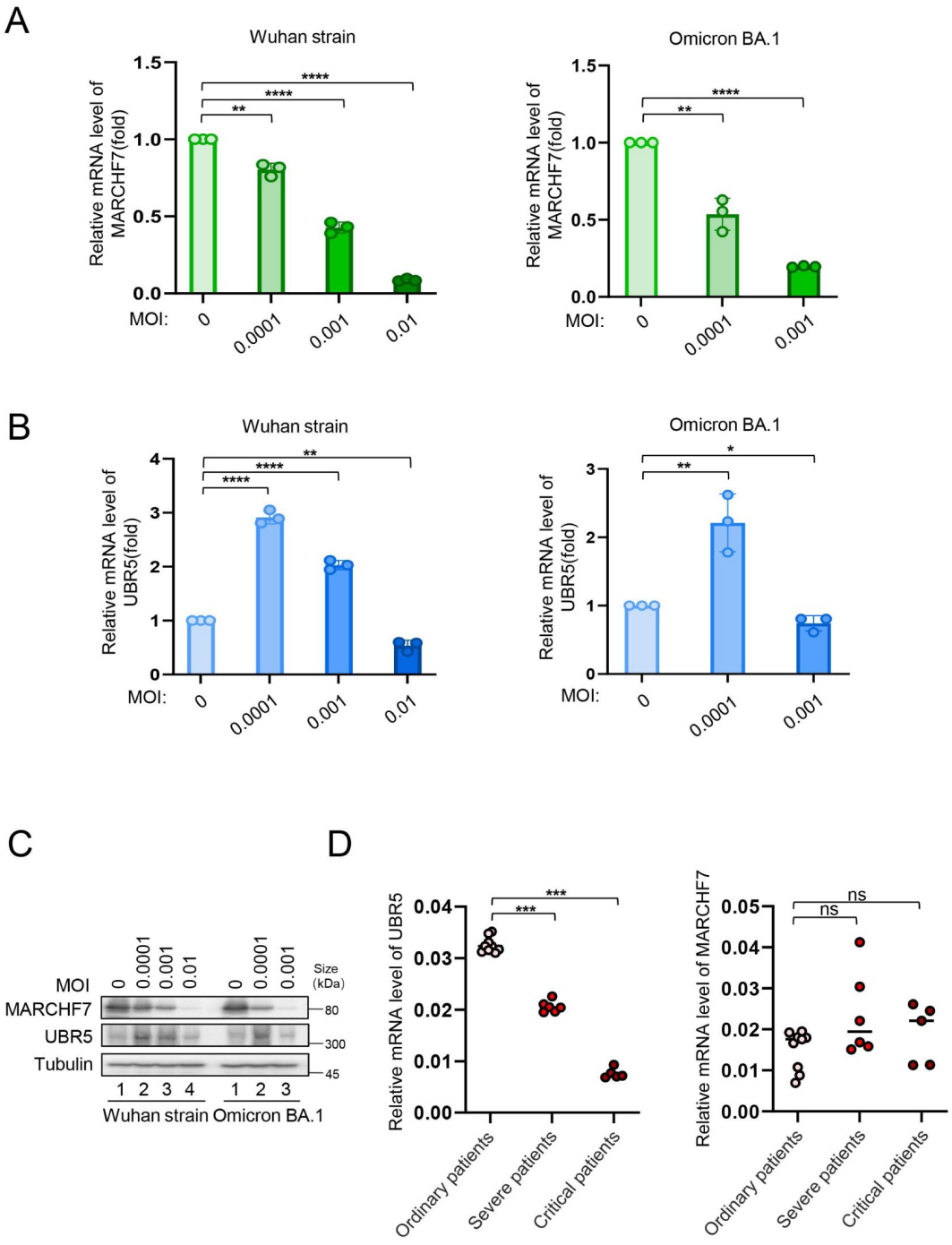

Figure 6 — figure supplement 4.

The expression level of MARCHF7 was negatively correlated with the viral titer, while the expression level of UBR5 was increased at low titer and decreased at high titer.

(A-C). The protein and mRNA levels of MARCHF7 or UBR5 upon infection with different titers. Endogenous MARCHF7 and UBR5 RNA levels were detected by RT-qPCR 48 hours after infection with different titers of Wuhan strain (MOI:0, 0.0001, 0.001, 0.01) or omicron BA.1 strain (MOI:0, 0.0001, 0.001). Protein levels were examined by IB.

D. The expression level of UBR5 was negatively correlated with the severity of the disease but MARCHF7 expression levels were not. PBMC cells were extracted from common, severe and critical COVID-19 patients. RT-qPCR was used to detect the mRNA level of UBR5 or MARCHF7 in patients. Significance was determined by one-way ANOVA, followed by a Tukey multiple comparisons posttest. ns, $P > 0.05$; **$P < 0.01$; ***$P < 0.001$.

Acknowledgements

We thank C.Y. Dai for providing critical reagents.

Additional information

Funding information

This work was supported by funding from the National Natural Science Foundation of China (82341072, 81930062 and 82272316 to ZWY, 82341062 to LZL), the National Key R&D Program of China (2021YFC2301900 and 2301904, 2023YFC2306603), the Science and Technology Department of Jilin Province (YDZJ202301ZYTS521 and YDZJ202201ZYTS587), the Key Laboratory of Molecular Virology, Jilin Province (20102209), and Bethune Project, Jilin University (2023B03). The funding sources were involved in study design, data collection and interpretation, and the decision to submit the work for publication.

Authors' contributions

L.T.: Conceptualization; Data curation; Formal Analysis; Investigation; Methodology; Writing – original draft. Z.Z.: Methodology; Data curation; Writing – review & editing. Z.L.: Conceptualization; Data curation; Formal Analysis; Investigation; Methodology; Writing – review & editing; Funding acquisition. X.L., Z.L. and W.G.: Methodology; Resources. W.Z.: Conceptualization; Formal Analysis; Funding acquisition; Methodology; Project administration; Resources; Writing – review & editing.

References

Balieiro A. M., Anunciação E. L., Costa C. H., Qayed W. S., Silva J. R. A (2022) **Computational Analysis of SAM Analogs as Methyltransferase Inhibitors of nsp16/nsp10 Complex from SARS-CoV-2** *International Journal of Molecular Sciences* **23**:13972

Banerjee A. K., Blanco M. R., Bruce E. A., Honson D. D., Chen L. M., Chow A., Bhat P., Ollikainen N., Quinodoz S. A., Loney C (2020) **SARS-CoV-2 disrupts splicing, translation, and protein trafficking to suppress host defenses** *Cell* **183**:1325–1339

Bonamassa B., Hai L., Liu D (2011) **Hydrodynamic gene delivery and its applications in pharmaceutical research** *Pharm Res* **28**:694–701 https://doi.org/10.1007/s11095-010-0338-9

Cai B., Zhao J., Zhang Y., Liu Y., Ma C., Yi F., Zheng Y., Zhang L., Chen T., Liu H (2022) **USP5 attenuates NLRP3 inflammasome activation by promoting autophagic degradation of NLRP3** *Autophagy* **18**:990–1004

Chen X., Tian L., Zhang L., Gao W., Yu M., Li Z., Zhang W. (2024) **Deubiquitinase USP39 promotes SARS-CoV-2 replication by deubiquitinating and stabilizing the envelope protein** *Antiviral Res* **221**:105790 https://doi.org/10.1016/j.antiviral.2023.105790

Decroly E., Debarnot C., Ferron F., Bouvet M., Coutard B., Imbert I., Gluais L., Papageorgiou N., Sharff A., Bricogne G (2011) **Crystal structure and functional analysis of the SARS-coronavirus RNA cap 2 ' -O-methyltransferase nsp10/nsp16 complex** *PLoS pathogens* **7**:e1002059

Fan L., Zhou Y., Wei X., Feng W., Guo H., Li Y., Gao X., Zhou J., Wen Y., Wu Y., Shen X., Liu L., Xu G., Zhang Z (2024) **The E3 ligase TRIM22 restricts SARS-CoV-2 replication by promoting proteasomal degradation of NSP8** *mBio* **15**:e0232023 https://doi.org/10.1128/mbio.02320-23

Gao W., Wang L., Cui W., Wang H., Huang G., Li Z., Li G., Zhang W (2024) **Deubiquitinase USP1 regulates sarbecovirus ORF6 protein function** *J Virol* **98**:e0143723 https://doi.org/10.1128/jvi.01437-23

Gao W., Wang L., Ju X., Zhao S., Li Z., Su M., Xu J., Wang P., Ding Q., Lv G (2022) **The deubiquitinase USP29 promotes SARS-CoV-2 virulence by preventing proteasome degradation of ORF9b** *Mbio* **13**:e01300–e01322

Grice G. L., Nathan J. A (2016) **The recognition of ubiquitinated proteins by the proteasome** *Cellular and molecular life sciences* **73**:3497

Guo G., Gao M., Gao X., Zhu B., Huang J., Luo K., Zhang Y., Sun J., Deng M., Lou Z (2021) **SARS-CoV-2 non-structural protein 13 (nsp13) hijacks host deubiquitinase USP13 and counteracts host antiviral immune response** *Signal transduction and targeted therapy* **6**:119

Hojyo S., Uchida M., Tanaka K., Hasebe R., Tanaka Y., Murakami M., Hirano T (2020) **How COVID-19 induces cytokine storm with high mortality** *Inflamm Regen* **40**:37 https://doi.org/10.1186/s41232-020-00146-3

Hu B., Huang S., Yin L (2021) **The cytokine storm and COVID-19** *J Med Virol* **93**:250–256 https://doi.org/10.1002/jmv.26232

Ju X., Zhu Y., Wang Y., Li J., Zhang J., Gong M., Ren W., Li S., Zhong J., Zhang L., Zhang Q. C., Zhang R., Ding Q (2021) **A novel cell culture system modeling the SARS-CoV-2 life cycle** *PLoS Pathog* **17**:e1009439 https://doi.org/10.1371/joumal.ppat.1009439

Kamimura K., Kanefuji T., Yokoo T., Abe H., Suda T., Kobayashi Y., Zhang G., Aoyagi Y., Liu D (2014) **Safety assessment of liver-targeted hydrodynamic gene delivery in dogs** *PLoS One* **9**:e107203 https://doi.org/10.1371/joumal.pone.0107203

Kim J. G., Shin H.-C., Seo T., Nawale L., Han G., Kim B. Y., Kim S. J., Cha-Molstad H (2021) **Signaling pathways regulated by UBR box-containing E3 ligases** *International journal of molecular sciences*

Klima M., Khalili Yazdi A., Li F., Chau I., Hajian T., Bolotokova A., Kaniskan H. Ü., Han Y., Wang K., Li D (2022) **Crystal structure of SARS-CoV-2 nsp10–nsp16 in complex with small molecule inhibitors, SS148 and WZ16** *Protein Science* **31**:e4395

Li Z., Hao P., Zhao Z., Gao W., Huan C., Li L., Chen X., Wang H., Jin N., Luo Z.-Q (2023) **The E3 ligase RNF5 restricts SARS-CoV-2 replication by targeting its envelope protein for degradation** *Signal Transduction and Targeted Therapy* **8**:53

Liang X., Xiao J., Li X., Liu Y., Lu Y., Wen Y., Li Z., Che X., Ma Y., Zhang X (2022) **A C-terminal glutamine recognition mechanism revealed by E3 ligase TRIM7 structures** *Nature Chemical Biology* **18**:1214–1223

Lin S., Chen H., Ye F., Chen Z., Yang F., Zheng Y., Cao Y., Qiao J., Yang S., Lu G (2020) **Crystal structure of SARS-CoV-2 nsp10/nsp16 2 '-O-methylase and its implication on antiviral drug design** *Signal transduction and targeted therapy* **5**:131

Lugari A., Betzi S., Decroly E., Bonnaud E., Hermant A., Guillemot J.-C., Debarnot C., Borg J.-P., Bouvet M., Canard B (2010) **Molecular mapping of the RNA Cap 2 ' -O-methyltransferase activation interface between severe acute respiratory syndrome coronavirus nsp10 and nsp16** *Journal of Biological Chemistry* **285**:33230–33241

Mahajan S., Sharma G. K., Bora K., Pattnaik B (2021) **Identification of novel interactions between host and non-structural protein 2C of foot-and-mouth disease virus** *J Gen Virol* **1023** https://doi.org/10.1099/jgv.0.001577

Maimaitiyiming Y., Yang T., Wang Q. Q., Feng Y., Chen Z., Björklund M., Wang F., Hu C., Hsu C.-H., Naranmandura H (2022) **Heat treatment promotes ubiquitin-mediated proteolysis of SARS-CoV-2 RNA polymerase and decreases viral load** *Research*

Makaremi S., Asgarzadeh A., Kianfar H., Mohammadnia A., Asghariazar V., Safarzadeh E (2022) **The role of IL-1 family of cytokines and receptors in pathogenesis of COVID-19** *Inflamm Res* **71**:923–947 https://doi.org/10.1007/s00011-022-01596-w

McClellan A. J., Laugesen S. H., Ellgaard L (2019) **Cellular functions and molecular mechanisms of non-lysine ubiquitination** *Open Biology* **9**:190147

Melo-Filho C. C., Bobrowski T., Martin H.-J., Sessions Z., Popov K. I., Moorman N. J., Baric R. S., Muratov E. N., Tropsha A (2022) **). Conserved coronavirus proteins as targets of broad-spectrum antivirals** *Antiviral Research* **204**:105360

Muñoz-Escobar J., Matta-Camacho E., Kozlov G., Gehring K (2015) **The MLLE domain of the ubiquitin ligase UBR5 binds to its catalytic domain to regulate substrate binding** *Journal of Biological Chemistry*

Nathan J. A., Sengupta S., Wood S. A., Admon A., Markson G., Sanderson C., Lehner P. J (2008) **The ubiquitin E3 ligase MARCH7 is differentially regulated by the deubiquitylating enzymes USP7 and USP9X** *Traffic*

Park G. J., Osinski A., Hernandez G., Eitson J. L., Majumdar A., Tonelli M., Henzler-Wildman K., Pawlowski K., Chen Z., Li Y (2022) **The mechanism of RNA capping by SARS-CoV-2** *Nature* **609**:793–800

Qiao X., Liu Y., Prada M. L., Mohan A. K., Gupta A., Jaiswal A., Sharma M., Merisaari J., Haikala H. M., Talvinen K (2020) **UBR5 is coamplified with MYC in breast tumors and encodes an ubiquitin ligase that limits MYC-dependent apoptosis** *Cancer research*

Raper S. E., Chirmule N., Lee F. S., Wivel N. A., Bagg A., Gao G. P., Wilson J. M., Batshaw M. L (2003) **). Fatal systemic inflammatory response syndrome in a ornithine transcarbamylase deficient patient following adenoviral gene transfer** *Mol Genet Metab* **80**:148–158 https://doi.org/10.1016/j.ymgme.2003.08.016

Rosas-Lemus M., Minasov G., Shuvalova L., Inniss N. L., Kiryukhina O., Brunzelle J., Satchell K. J (2020) **High-resolution structures of the SARS-CoV-2 2'-O-methyltransferase reveal strategies for structure-based inhibitor design** *Science signaling* **13**:eabe1202

Russ A., Wittmann S., Tsukamoto Y., Herrmann A., Deutschmann J., Lagisquet J., Ensser A., Kato H., Gramberg T (2022) **Nsp16 shields SARS–CoV-2 from efficient MDA5 sensing and IFIT1-mediated restriction** *EMBO reports* **23**:e55648

Shearer R. F., Frikstad K.-A. M., McKenna J., McCloy R. A., Deng N., Burgess A., Stokke T., Patzke S., Saunders D. N (2018) **The E3 ubiquitin ligase UBR5 regulates centriolar satellite stability and primary cilia** *Molecular biology of the cell*

Song P., Li W., Xie J., Hou Y., You C (2020) **Cytokine storm induced by SARS-CoV-2** *Clin Chim Acta* https://doi.org/10.1016/j.cca.2020.06.017

Suda T., Yokoo T., Kanefuji T., Kamimura K., Zhang G., Liu D (2023) **Hydrodynamic Delivery: Characteristics, Applications, and Technological Advances** *Pharmaceutics* **15** https://doi.org/10.3390/pharmaceutics15041111

Wu B., Song M., Dong Q., Xiang G., Li J., Ma X., Wei F (2022) **UBR5 promotes tumor immune evasion through enhancing IFN-γ-induced PDL1 transcription in triple negative breast cancer** *Theranostics*

Xiang G., Wang S., Chen L., Song M., Song X., Wang H., Zhou P., Ma X., Yu J (2022) **UBR5 targets tumor suppressor CDC73 proteolytically to promote aggressive breast cancer** *Cell Death & Disease* **13**:451

Xu G., Wu Y., Xiao T., Qi F., Fan L., Zhang S., Zhou J., He Y., Gao X., Zeng H (2022) **Multiomics approach reveals the ubiquitination-specific processes hijacked by SARS-CoV-2** *Signal Transduction and Targeted Therapy* **7**:312

Zhang H., Zheng H., Zhu J., Dong Q., Wang J., Fan H., Chen Y., Zhang X., Han X., Li Q (2021) **Ubiquitin-modified proteome of SARS-CoV-2-infected host cells reveals insights into**

virus–host interaction and pathogenesis *Journal of Proteome Research* **20**:2224–2239

Zhang J., Cruz-Cosme R., Zhuang M.-W., Liu D., Liu Y., Teng S., Wang P.-H., Tang Q (2020) **A systemic and molecular study of subcellular localization of SARS-CoV-2 proteins** *Signal transduction and targeted therapy* **5**:269

Zhang L., Hao P., Chen X., Lv S., Gao W., Li C., Li Z., Zhang W (2024) **CRL4B E3 ligase recruited by PRPF19 inhibits SARS-CoV-2 infection by targeting ORF6 for ubiquitin-dependent degradation** *mBio* **15**:e0307123 https://doi.org/10.1128/mbio.03071-23

Zhang L., Wang H., Tian L., Li H (2016) **Expression of USP7 and MARCH7 is correlated with poor prognosis in epithelial ovarian cancer** *The Tohoku journal of experimental medicine* **239**:165–175

Zhang X., Yang Z., Pan T., Sun Q., Chen Q., Wang P. H., Li X., Kuang E (2023) **SARS-CoV-2 Nsp8 suppresses MDA5 antiviral immune responses by impairing TRIM4-mediated K63-linked polyubiquitination** *PLoS Pathog* **19**:e1011792 https://doi.org/10.1371/joumal.ppat.1011792

Zhao K., Yang Y., Zhang G., Wang C., Wang D., Wu M., Mei Y (2018) **Regulation of the Mdm2–p53 pathway by the ubiquitin E3 ligase MARCH 7** *EMBO reports* **19**:305–319

Zheng C (2021) **The emerging roles of the MARCH ligases in antiviral innate immunity** *International Journal of Biological Macromolecules* **171**:423–427

Zhou Y., Zheng R., Liu D., Liu S., Disoma C., Li S., Liao Y., Chen Z., Du A., Dong Z (2022) **UBR5 Acts as an Antiviral Host Factor against MERS-CoV via Promoting Ubiquitination and Degradation of ORF4b** *Journal of Virology* **96**:e00741–722

Züst R., Cervantes-Barragan L., Habjan M., Maier R., Neuman B. W., Ziebuhr J., Szretter K. J., Baker S. C., Barchet W., Diamond M. S (2011) **Ribose 2'-O-methylation provides a molecular signature for the distinction of self and non-self mRNA dependent on the RNA sensor Mda5** *Nature immunology* **12**:137–143

Author information

Li Tian[#]

Department of Infectious Diseases, Infectious Diseases and Pathogen Biology Center, Institute of Virology and AIDS Research, Key Laboratory of Organ Regeneration and Transplantation of The Ministry of Education, The First Hospital of Jilin University, Changchun, China

[#]These authors contributed equally to this article.

Zongzheng Zhao[#]

Research Unit of Key Technologies for Prevention and Control of Virus Zoonoses, Chinese Academy of Medical Sciences, Changchun Veterinary Research Institute, Chinese Academy of Agricultural Sciences, Changchun, China

[#]These authors contributed equally to this article.

Wenying Gao
Department of Infectious Diseases, Infectious Diseases and Pathogen Biology Center, Institute of Virology and AIDS Research, Key Laboratory of Organ Regeneration and Transplantation of The Ministry of Education, The First Hospital of Jilin University, Changchun, China

Zirui Liu
Research Unit of Key Technologies for Prevention and Control of Virus Zoonoses, Chinese Academy of Medical Sciences, Changchun Veterinary Research Institute, Chinese Academy of Agricultural Sciences, Changchun, China

Xiao Li
Research Unit of Key Technologies for Prevention and Control of Virus Zoonoses, Chinese Academy of Medical Sciences, Changchun Veterinary Research Institute, Chinese Academy of Agricultural Sciences, Changchun, China

For correspondence: skylee6226@163.com

Wenyan Zhang
Department of Infectious Diseases, Infectious Diseases and Pathogen Biology Center, Institute of Virology and AIDS Research, Key Laboratory of Organ Regeneration and Transplantation of The Ministry of Education, The First Hospital of Jilin University, Changchun, China
ORCID iD: 0000-0003-4507-521X

For correspondence: zhangwenyan@jlu.edu.cn

Zhaolong Li
Department of Infectious Diseases, Infectious Diseases and Pathogen Biology Center, Institute of Virology and AIDS Research, Key Laboratory of Organ Regeneration and Transplantation of The Ministry of Education, The First Hospital of Jilin University, Changchun, China

For correspondence: lizhaolong@jlu.edu.cn

Editors

Reviewing Editor
Craig Wilen
Yale School of Medicine, New Haven, United States of America

Senior Editor
John Schoggins
The University of Texas Southwestern Medical Center, Dallas, United States of America

Reviewer #1 (Public review):

In this study, Tiang et al. explore the role of ubiquitination of non-structural protein 16 (nsp16) in the SARS-CoV-2 life cycle. nsp16, in conjunction with nsp10, performs the final step of viral mRNA capping through its 2'-O-methylase activity. This modification allows the virus to evade host immune responses and protects its mRNA from degradation. The authors demonstrate that nsp16 undergoes ubiquitination and subsequent degradation by the host E3 ubiquitin ligases UBR5 and MARCHF7 via the ubiquitin-proteasome system (UPS). Specifically, UBR5 and MARCHF7 mediate nsp16 degradation through K48- and K27-linked ubiquitination, respectively. Notably, degradation of nsp16 by either UBR5 or MARCHF7 operates

independently, with both mechanisms effectively inhibiting SARS-CoV-2 replication in vitro and in vivo. Furthermore, UBR5 and MARCHF7 exhibit broad-spectrum antiviral activity by targeting nsp16 variants from various SARS-CoV-2 strains. This research advances our understanding of how nsp16 ubiquitination impacts viral replication and highlights potential targets for developing broadly effective antiviral therapies.

Strengths:

The proposed study is of significant interest to the virology community because it aims to elucidate the biological role of ubiquitination in coronavirus proteins and its impact on the viral life cycle. Understanding these mechanisms will address broadly applicable questions about coronavirus biology and enhance our overall knowledge of ubiquitination's diverse functions in cell biology. Employing in vivo studies is a strength.

Weaknesses:

Minor comments:
Figure 5A- The authors should ensure that the figure is properly labeled to clearly distinguish between the IP (Immunoprecipitation) panel and the input panel.

https://doi.org/10.7554/eLife.102277.2.sa2

Reviewer #3 (Public review):

Summary:

The manuscript "SARS-CoV-2 nsp16 is regulated by host E3 ubiquitin ligases, UBR5 and MARCHF7" is an interesting work by Tian et al. describing the degradation/ stability of NSP16 of SARS CoV2 via K48 and K27-linked Ubiquitination and proteasomal degradation. The authors have demonstrated that UBR5 and MARCHF7, an E3 ubiquitin ligase bring about the ubiquitination of NSP16. The concept, and experimental approach to prove the hypothesis looks ok. The in vivo data looks ok with the controls. Overall, the manuscript is good.

Strengths:

The study identified important E3 ligases (MARCHF7 and UBR5) that can ubiquitinate NSP16, an important viral factor.

Comments on revisions:

I had gone through the revised form of the manuscript thoroughly. The authors have addressed all of my concerns. To me, the experimental approach looks convincing that the host E3 ubiquitin ligases (UBR5 and MARCHF7) ubiquitinate NSP16 and mark it for proteasomal degradation via K48- and K27- linkage. The authors have represented the final figure (Fig.8) in a convincing manner, opening a new window to explore the mechanism of capping the vRNA bu NSP16.

https://doi.org/10.7554/eLife.102277.2.sa1

Author response:

The following is the authors' response to the original reviews.

> ***Reviewer #1 (Public review):***
>
> *Major comments:*

> *(1) In Figure 1 the authors could reference and use NSP8 (PMID: 38275298) and Nucleocapsid (PMID: 37185839) in their experiments as positive controls.*

Thank you for your suggestion! In Figure 1A, during our screening of SARS-CoV-2 nsp proteins regulated by MG132, we confirmed that nsp8 can also be restored by MG132. This finding indicates that nsp8 is degraded via the proteasome pathway and can therefore serve as a positive control for the experiment. It has been reported that nsp8 undergoes degradation via the ubiquitin-proteasome pathway following its ubiquitination mediated by TRIM22. We have added the description at line 115 in the manuscript.

> *(2) The data indicating that NSP16 is ubiquitinated come from overexpression systems, and it is possible that NSP16 ubiquitination only occurs in expression contexts, not during coronavirus infection. If NSP16 ubiquitination can't be measured in the context of infection, it is unclear how we can make any conclusions. The authors need to demonstrate the ubiquitination of NSP16 in the context of viral infection.*

We greatly appreciate the reviewer's suggestion and have incorporated the corresponding experimental results. As shown in Figure 5A, co-IP experiments using an endogenous nsp16 antibody were conducted following infection with the SARS-CoV-2 Wuhan strain. These experiments confirmed that the nsp16 protein encoded by the virus undergoes ubiquitination in infected cells. This finding highlights the ubiquitination of nsp16 within a biological context, thereby supporting our conclusions in expression contexts.

> *(3) In Figure 4, adding controls will strengthen the authors' conclusion.*
>
> *a) Is it possible to observe ubiquitination of NSP16 by transfecting in NSP16-FLAG tagged, immunoprecipitate NSP16, run a western blot, and probe for endogenous ubiquitin?*
>
> *b) Can the authors please include an empty vector control as well as WT ubiquitin in these panels for comparison?*
>
> *c) In addition, why are the Ubiquitination patterns different in the IP panels of D and E vs B?? Without an empty vector control, it is challenging to conclude what the background is.*

Thank you for your valuable suggestions! We have made the following changes and additions in response to your comments:

a) We have conducted the experiments as per the reviewer's suggestion. Figure 3B shows the result. Co-IP experiments were performed, and endogenous ubiquitination of nsp16 was observed using the endogenous ubiquitin antibody.

b) We apologize for previously focusing solely on presenting multiple ubiquitin mutants on a single panel of nsp16 IP without considering the inclusion of an empty vector control and WT ubiquitin. The experiment has been redesigned and conducted, and the results are now presented in Figures 3E and 3F.

c) The differences in the ubiquitination patterns observed between the IP panels in Figures 3E and 3F compared to 3C may be due to varying plasmids, differences in antibody and depth of exposure. To address this, we have standardized the plasmids in the figure and included an empty vector control as a negative control to clarify the background signal.

> *(4) Overexpression of the ubiquitin mutants may have an indirect effect on protein homeostasis. The authors can also utilize linkage-specific antibodies in their studies to elucidate the ubiquitin linkage associated with NSP16 ubiquitination. K63-linkage Specific*

> *Polyubiquitin (D7A11) Rabbit mAb, 5621S, and K48-linkage Specific Polyubiquitin (D9D5) Rabbit mAb, 8081S from Cell Signaling Technologies?*

We greatly appreciate the reviewer's excellent suggestion! Using linkage-specific antibodies to elucidate the ubiquitin linkage associated with nsp16 ubiquitination would indeed provide more direct evidence. However, due to the long lead time for obtaining these antibodies, we plan to conduct further verification in future experiments.

> *(5) The authors discussed the subcellular localization of overexpressed NSP16- showing the localization of NSP16 in the context of viral infection would strengthen the study. If this is challenging, can the authors express NSP16 along with the co-factor NSP10 and examine its subcellular localization?*

Thank you for your suggestion! During viral infection, we observed the ubiquitination of the nsp16 protein through co-IP experiments, indicating that the presence of nsp10 does not influence the regulation of nsp16 ubiquitination by MARCHF7 or UBR5 (Figure 5A). Therefore, we believe that investigating the co-localization of nsp10 and nsp16 would not provide additional value to our results. Additionally, through a literature review, we found studies that have already examined the localization of nsp10 and nsp16 following viral infection. These studies revealed that nsp10 was located in the cytoplasm, while nsp16 can be detected in both the nucleus and cytoplasm (PMID: 33080218; PMID: 34452352). This observation is consistent with the localization of nsp16 that we observed in our overexpression experiments.

> *(6) a) In Figure 3A, the authors should note that the interaction of NPS16 appears weak with UBR5. The authors should confirm that the interaction of NSP16 and the E3 ligases is relevant in the context of viral infection.*
>
> *b) In Figure 3B, the scale bars should be labeled in at least one panel, as well as in the legend.*
>
> *c) The authors discussed nuclear localization of MARCHF7, UBR5, and NSP16, therefore a control with a nuclear stain should be included in this figure to enhance the study.*
>
> *d) Some panels look overexposed while others are blurry which decreases the robustness of the interaction as the authors stated in line 191. To strengthen the results of Figure 3, consider GST purification and in vitro, cell-free binding assays to confirm a direct interaction between nsp16 and the E3 ligases*

Thank you for the reviewer's thoughtful suggestions! We have made the following changes and adjustments based on your recommendations:

a) On the interaction between nsp16 and UBR5:

The interaction between nsp16 and UBR5 appears to be weak, possibly due to the large size of the UBR5 protein (300 kDa). As a result, there are challenges in presenting the experimental results, including difficulties in both expression and protein level detection. To further confirm the relevance of the interaction between nsp16 and the E3 ligases in the context of viral infection, we have performed experiments, and the results are presented in Figure 5A.

b) On scale bars:

The issue regarding the scale bars in Figure 4 has been addressed, and we have now included them in the figure legend for clarity (Line 885).

c) On nuclear localization control:

For the localization of MARCHF7, UBR5, and nsp16 in Figure 4C, given that both MARCHF7 and UBR5 are tagged with CFP, DAPI staining would result in spectral overlap. However, we conducted co-localization experiments for MARCHF7 or UBR5 with nsp16 in Figure 4—figure supplements 1E and 1F, where DAPI staining was included to illustrate the localization of these three proteins. Our experiments showed that while these proteins are present in both the nucleus and cytoplasm, they are predominantly localized in the cytoplasm.

d) On validation of direct interaction:

We attempted GST purification and in vitro cell-free binding assays to verify the direct interaction between nsp16 and the E3 ligases. However, UBR5 and MARCHF7 are both large proteins, with UBR5 being particularly large, which significantly increased the difficulty of purification. Additionally, we faced challenges in purifying nsp16, as the purified nsp16 protein tended to aggregate. We will continue to optimize purification techniques and conditions in future experiments.

We appreciate your valuable comments, which have greatly contributed to improving our experiments and conclusions.

> *(7) To confirm the knockdown of the E3 ligases by siRNA, the authors should use western blotting to show the presence/absence/decrease of the protein levels in addition to mRNA levels by RT-PCR. The authors have the lysates, and they have shown that the antibodies for MARCHF7 and UBR5 work therefore including this throughout the manuscript to help substantiate the authors' conclusions.*

Thank you for the reviewer's valuable suggestion! We have validated the knockdown efficiency at the protein level for the experiments involving siRNA knockdown. Corresponding Western blot images are now included in the relevant experiments to substantiate our conclusions, in addition to the RT-PCR data, including Figures 2, 4 and 5.

> *(8) In the overexpression studies of the E3 ligases with viral infection in Figure 5, the authors should include the catalytic mutants for the E3 ligases with the nsp16 gradient experiment. This would strengthen the conclusion of the studies.*

Thank you for the reviewer's suggestion! We have conducted the relevant experiments based on your recommendation, and the corresponding data are presented in the Figure 6—figure supplements 2A-H. These results strengthen the conclusions of our study.

> *(9) Figure 5: For C and F, for a better comparison of the efficacy against the 2 strains, the authors should use the same scale. This could benefit from a kinetics experiment.*

Thank you for the reviewer's suggestion! We have made revisions in Figures 5E and 5H in responses to your recommendation.

> *(10) Is there a synergistic effect of double E3 knockdown on viral replication?*

Thank you for the reviewer's question! In Figures 5—figure supplement 1A-B, we conducted experiments by individually and simultaneously knocking down MARCHF7 or UBR5, followed by infection with viral SARS-CoV-2 transmissible virus-like particles. The results revealed that simultaneous knockdown further enhances viral replication, demonstrating a synergistic effect.

> *(11) In lines 98-100 the authors state "This dual targeting by MARCHF7 and UBR5 impairs the 2'-O-MTase activity of nsp16, blocking the conversion of cap-0 to cap-1 at the 5 'end*

> *of viral RNA, ultimately exhibiting potent antiviral activity against SARS-CoV-2". The authors did not examine the 2'-O-MTase activity of nsp16. The authors should rephrase this or provide the data if this experiment was done.*

Thank you for the reviewer's valuable suggestion! Based on your comment, we have revised the ambiguous wording located in lines 100-104.

> *(12) In the discussion, the authors reported that elucidating a specific lysine residue (s) that is ubiquitinated was challenging and stated that they generated multiple mutants including truncated mutants, and wrote "data not shown". The authors need to include this data as supplementary.*

Thank you for the reviewer's suggestion! Based on your comment, we have included the data regarding the specific lysine residue(s) that is ubiquitinated, along with the truncated mutants, as supplementary data (Appendix-figure S2).

> *(13) In Figure 7, the authors showed a copy number of SARS CoV-2 E in lung tissue. The authors should show viral titers using either the plaque assay or the TCID50 assay.*

Thank you for the reviewer's suggestion! Based on your comment, we measured the TCID50 of the virus in the lung tissue homogenates, and the results are presented in Figure 7D.

> *Minor comments:*
>
> *(1) Line 76: while many E3 ubiquitin ligases directly recognize and bind to their target substrates, cullin-RING ligases directly bind an adaptor, which binds a substrate receptor and/or the substrate directly, while the RING-box protein binds a different surface of the cullin and is also not directly interacting with substrate.*

Thank you for the reviewer's valuable suggestion! Based on your comment, we have revised the ambiguous wording in line 76.

> *(2) Line 161: having introduced the suggestion that NSP16 is ubiquitinated by these ligases, consider moving Figure 4 to the Figure 3 spot.*

Based on your comment, we have rearranged the order of the figures and moved Figure 4 to the Figure 3 spot.

> *(3) Figure 2: Can the authors please do +/- MG132 for each siRNA? It is possible that the lanes where we don't see NSP16 were because there was no NSP16 expressed, OR it was degraded, MG132 would confirm one or the other.*

Thank you for the reviewer's suggestion! Based on your comment, we have redesigned the experiment and included the MG132 treatment for each siRNA. The results are presented in Figure 2A.

> *(4) Line 165: The authors write "As confirmed by MS, both Myc-tagged MARCHF7 and endogenous UBR5 interact with nsp16, as seen in the Co-IP experiment" should be the reverse, MS suggests NSP16-E3 interaction, the co-ip confirms this.*

Based on your comment, we have revised the wording in line 183 to ensure accuracy. MS suggests the interaction between nsp16 and the E3 ligases, while the Co-IP experiment confirms this interaction.

> *(5) Line 178: the cited paper doesn't clearly show NSP16 nuclear localization, nor do the authors of said paper claim that they found it there. It is cytoplasmic. Additionally, said paper used overexpression, and it is unclear if NSP16 is nuclear in the context of viral infection.*

Thank you for the reviewer's suggestion! The referenced paper states, "As can be seen in the Supplementary Fig. S2, the viral proteins are either cytoplasmic (NSP2, NSP3C, NSP4, NSP8, Spike, M, N, ORF3a, ORF3b, ORF6, ORF7a, ORF7b, ORF8, ORF9b, and ORF10) or both nuclear and cytoplasmic (NSP1, NSP3N, NSP5, NSP6, NSP7, NSP9, NSP10, NSP12, NSP13, NSP14, NSP15, NSP16, E, and ORF9a)," indicating that nsp16 is localized in both the nucleus and cytoplasm. Upon reviewing the literature, we found that the paper (PMID: 33080218) reports the distribution of nsp16 protein following viral infection. The results indicate that nsp16 is present in both the nucleus and cytoplasm, although the authors of the referenced paper claim that ns16 was located in the nucleus.

> *(6) Line 197: in addition to the 7 lysine residues, ubiquitin can also form linear N-terminal linkages.*

Thank you for the reviewer's suggestion! Linear N-terminal ubiquitination, with its distinct linkage and substrate recognition mechanism, is typically mediated by a complex consisting of the E3 ubiquitin ligases HOIL-1 and HOIP, and differs from classical ubiquitination. Therefore, this type of ubiquitin chain was not investigated in our experiments.

> *(7) Line 202: Authors state "Interestingly, all single-lysine Ub mutants promoted nsp16 ubiquitylation to varying degrees, indicating a complex polyubiquitin chain structure on nsp16 potentially regulated by multiple E3 ligases". However, not all the mutants. K33 isn't supported by the blot.*

Thank you for pointing that out! Indeed, we made an error in our description. The K33 mutant did not promote nsp16 ubiquitylation, and we have corrected this in the manuscript accordingly in line 173.

> *(8) Line 204: consider including "E2-E3 ligase pairs" for RING ligases the E2 determines the linkage type see: Cell Research (2016) 26:423-440.*

Thank you for your suggestion! We have included the term "E2-E3 ligase pairs" in the article in line 176.

> *(9) Line 235: The authors used the real virus, the inclusion of the BLS2 virus here is extraneous, it doesn't add anything. The authors can consider removing it.*

Thank you for your suggestion! In our experiments, we performed simultaneous knockdown of two E3 ligases, so we believe this data is relevant and should not be removed.

> *(10) Line 238: Authors state: "led to a significant increase in SARS-CoV-2 levels compared to the control group". What is meant by "levels?"*

Thank you for your careful reading. We have updated "levels" to "replication" as suggested to clarify the meaning in line 237.

> *(11) Line 245: increased titers. This could be improved for specificity by saying, 1-log increase for example.*

Thank you for the reviewer's valuable suggestions. We have made the necessary changes and specified "increased titers" as a "1-log increase" in lines 249 and 261.

> *(12) Line 249: in Figure 5H again, the authors are showing relative mRNA levels. Ideally should show protein levels by western blot.*

Thank you for the reviewer's suggestion! We have performed protein-level detection of the knockdown efficiency for the samples, and the bands have been placed in the corresponding positions in Figure 5I.

> *(13) Line 259: "strongly linked to their ability to modulate..." This appears to be an overextension of the data. The data show nsp16 levels can compensate for E3 overexpression, but not that the E3 ligases are modulating this activity. We can infer this from previous experiments. Perhaps increasing the NSP12 levels would also have the same effect as they don't show that this is specific to NSP16. What about a catalytically dead E3?*

Thank you for the reviewer's thoughtful suggestion. We have revised the wording accordingly and designed the viral-related experiments with E3 enzyme activity mutants in Figure 6 supplement 2.

> *(14) Figure 6: In panel H the MW for UBR5 is incorrect, should be around 300kDa.*

Thank you for the reviewer's detailed suggestions. We have made the necessary revisions in Figure 6H.

> *(15) Line 267: "suggesting a more conserved sequence". What are the authors referring to? More conserved than what? This section would benefit from a discussion of which residues are mutated. Are they potential Ub sites, which could point to differential degradation by the E3s as due to more ubiquitination? Or rather to more efficient interaction with the E3? Is this conserved in related CoVs: original SARS and MERS, for instance?*

Thank you for the reviewer’s detailed suggestions. In this context, by “conservation,” we refer to the relative conservation of nsp16 proteins across different subtypes of the Omicron variant. We found that most of the mutation sites contained only 1 to 2 mutations. Additionally, we have constructed and validated multiple-mutant nsp16 proteins, which are still degraded by MARCHF7 or UBR5. Given the ongoing prevalence of the Omicron variant, we aim to explore the broad-spectrum degradation and antiviral effects of these two E3 ligases. While it would be ideal if these experiments could aid in identifying the ubiquitination sites, we have not yet identified any mutant forms that escape degradation. We also compared the nsp16 proteins of several other coronaviruses (such as human coronaviruses 229E, HKU1, MERS-CoV, NL63, OC43, and SARS-CoV-1), and found that these viruses' nsp16 proteins are not highly conserved. As a result, we have not further investigated whether MARCHF7 or UBR5 regulate the nsp16 proteins of these viruses.

> *(16) Line 347: 2C of what virus?*

Thank you for the reviewer’s careful reading. We have made the necessary additions to address this point in line 357.

> *(17) Line 890: "Scale bars, 25 mm". Should it be 25nm?*

Thank you for your feedback! I realized there was an error in the unit labeling, and I have corrected the relevant sections in line 904. I appreciate your careful reading.

> ***Reviewer #2 (Recommendations for the authors):***
>
> *(1) In Figure 6, the authors found that increasing amounts of nsp16 restored the replication of SARS-CoV-2 in the presence of MARCHF7 or UBR5. The authors better discuss the possibility that nsp16 may stimulate viral replication regardless of these E3 ligases, or provide evidence to further clarify this.*

Thank you for your thoughtful suggestion! Given the strong functionality of nsp16 itself, your consideration is very comprehensive. In Figure 6—figure supplement 2A–H, we conducted transfection experiments with E3 activity-deficient proteins and reintroduced nsp16. The results showed that, in the absence of active MARCHF7 or UBR5 antiviral function, overexpression of nsp16 did not promote viral replication, although the RNA levels of the M protein slightly increased. Therefore, in our experiments, excess nsp16 did not significantly stimulate viral replication.

> *(2) In Figure 7, the in vivo data supports the function of both E3 ligases to reduce viral infectivity. Is it possible that tail vein injection of naked plasmid DNA may stimulate the innate immune system, e.g., induce IFN as a DNA vaccine, which may contribute to the inhibitory effect? The authors are suggested to discuss or address it.*

Upon reviewing the relevant literature, we found that the hydrodynamic gene delivery (HGD) method using naked DNA is both highly efficient and associated with a low risk of triggering immune responses or oncogenesis. Studies have shown that HGD only weakly activates host immunity (reference: 37111597), which is less of a concern compared to other gene delivery methods. Although some studies have reported strong immune responses following the injection of naked DNA (e.g., Otc cDNA) in human trials, it is noteworthy that no such responses were observed in 17 other participants. This suggests that the immune reactions observed in some cases may be due to individual variability or limitations in animal models, which may not fully translate to human trials.

Based on these findings, we believe that the antiviral effects observed in our study are primarily attributable to the intrinsic properties and functions of the E3 ligases. Furthermore, it has been reported that mice and non-human primates exhibit significantly greater resistance to innate immune activation compared to humans. This highlights the challenges in translating these findings into effective antiviral therapeutics and underscores the need for further research in this area. We have incorporated the requested discussion into the manuscript in lines 393-410.

> *(3) The authors shall include some of the key data in supplementary figures in the main text, such as the study on UBR5 and MARCHF7 mediate broad-spectrum degradation of nsp16 variants and SARS-CoV-2 infection decreases UBR5 and MARCHF7 expression, which make it easier for readers to follow.*

Thank you for your valuable suggestion regarding the organization of our manuscript. In response to your feedback, we have moved the study on nsp16 variants to the Figure 6—figure supplement 3. Additionally, the data showing changes in UBR5 and MARCHF7 levels following viral infection have been added as supplementary data in Figure 6—figure supplement 4.

> *(4) The diagrammatic sketches in Figures 1E, S1A and B, 7A, and 8 had low resolutions. Please change them to higher resolutions. Moreover, please state the licensing rights of*

> *these diagrammatic sketches.*

Thank you for your detailed review! In response to your comment, we have improved the resolution of Figures 1E, S1A and B, 7A, and 8. Additionally, we have specified the drawing tools and source websites in the figure legends (lines 794, 813, 999, and 1013). And we have obtained the necessary licenses for each diagram.

Figure 1E: Created in BioRender. Li, Z. (2025) https://BioRender.com/h43f612

Figure S1B: Created in BioRender. Li, Z. (2025) https://BioRender.com/b98t559

Figure 7A: Created in BioRender. Li, Z. (2025) https://BioRender.com/e76g512

Figure 8: Created in BioRender. Li, Z. (2025) https://BioRender.com/o84p897

> *(5) The authors suggested that both UBR5 and MARCHF7 had a function in triggering the degradation of NSP16, however, the expression of UBR5 but not MARCHF7 was shown to be associated with the severity of clinical symptoms. Further, why did the host evolve 2 kinds of E3 ligases to adjust only 1 viral target? Please discuss them.*

Thank you for your insightful comments. We acknowledge that the limited number of patients with varying degrees of illness in our study could potentially mask some of the observed phenomena. Additionally, individual variability may also play a significant role, which highlights the challenges in translating findings from animal models to human trials.

Regarding the presence of two E3 ligases targeting the same substrate, we view this as part of an evolutionary arms race between the host and the virus. Viruses evolve mechanisms to counteract the host's antiviral responses, while the host, in turn, develops multiple pathways and strategies to combat viral infection. This dynamic may explain why multiple E3 ligases regulate the levels of the same factor, reflecting the host's complex and redundant antiviral defense mechanisms. We have incorporated the requested discussion into the manuscript in lines 359-362.

> *(6) Please standardize the symbol size of the bar charts in the same figure, just like in Figures 1D and 5.*

Thank you for your constructive suggestion. We have standardized the symbol sizes of the bar charts in the figure as per your recommendation, ensuring consistency across all panels.

> *(7) The use of English could be improved.*

Thank you for your feedback regarding the language. We have carefully reviewed the manuscript and made revisions to improve the clarity and fluency of the English.

> ***Reviewer #3 (Recommendations for the authors):***
>
> *Major points:*
>
> *(1) In Figure 1: The expression level of NSP6, 10, 11, and 12 is weak. Include a higher exposure blot (right next to these blots marking as higher exposure) to show the expression of these plasmids. Here, the NSP12 plasmid has no expression, so it is difficult to conclude the effect of MG132 from this blot. It will be appropriate to show the molecular weight of each gene fragment since some of the plasmids have multiple bands. Verify the densitometric analysis, the NSP4 (+/- MG132) blot, and the densitometric analysis do not correlate. Figure 1B: It is recommended to include appropriate control (media only) for NH4Cl. The DMSO control serves well for the drugs,*

> *not for Ammonium Chloride. In Figure 1C, how did the authors arrive at the 15-hour time point? The correlation does not appear as the authors claim. Where is the 15-hour sampling time point for MG132 or CHX chase? The experimental approach to screen the E2/E3 Ub ligase is appreciated.*

Thank you for your valuable feedback! Regarding your questions, we have made the following revisions:

On the expression of nsp6, nsp10, nsp11, and nsp12 in Figure 1:

We have replaced the blots for nsp10, nsp11, and nsp12 with higher exposure blots. However, due to the strong expression of NSP14, we were unable to generate a higher exposure blot for nsp6. Based on the current exposure, it is clear that nsp6 is not regulated by the proteasome. Additionally, in the high-exposure blot for nsp12, we were able to observe its expression and found that this protein is weakly regulated by MG132. Following your suggestion, we have labeled the molecular weights of the proteins in the figure.

On the densitometric analysis of nsp4 protein:

We recalculated the densitometric analysis for nsp4 and found no issues. Although the band intensities do not show large changes, the relative fold changes appear more pronounced because we normalized the data using GAPDH as an internal control. We have added detailed description in the figure legend.

On the NH4Cl control:

In this experiment, ammonium chloride was dissolved in DMSO. We reviewed the solubility data and found that ammonium chloride has a solubility of 50 mg/ml in DMSO, which is sufficient to reach the concentrations used in our experiment. While the solubility is higher in water, we believe that DMSO is an appropriate solvent for this compound in our context.

On the 15-hour time point in Figure 1C:

Regarding the 15-hour time point mentioned in Figure 1C, we did not collect samples at that time. We performed semi-quantitative analysis of protein levels at different time points using ImageJ and estimated the half-life time point based on the half-life calculation formula. Thank you for your suggestion; we will clarify this in the figure legend.

Once again, thank you for your thoughtful review and constructive suggestions. We have made the necessary revisions and improvements to the figures based on your feedback.

> *(2) In Figure 2: I do not find a reason to include DMSO control in the siRNAs for E2/E3 Ub. Please justify why it is necessary. It is requested to include WB for the siRNA-treated samples. It is strongly recommended to show the WB data for siRNA-treated samples because you are showing siRNA treatment of MARCHF7 in shUBR5 cells and vice versa. However, if antibodies for corresponding targets are not available, qPCR can be shown in graphical representation in supplementary data indicating the siRNA target region and qPCR target. Show a graphical representation of domains/ deleted regions of MARCHF7 and UBR5.*

Thank you for your valuable feedback! We have addressed your concerns as follows:

On the inclusion of the DMSO control group:

The DMSO group was initially included as a control for the MG132-treated group. By comparing with the MG132 group, we aimed to observe whether nsp16 levels were restored by MG132 treatment. Additionally, in siRNA knockdown experiments, the DMSO group was

included to compare nsp16 protein levels after knockdown with those in the NC group, as well as to assess differences in nsp16 restoration between MG132 treatment and factor knockdown. However, we acknowledge some issues in the control design. To address this, we have redesigned and conducted the experiments with improved controls (Figure 2A).

On validating knockdown efficiency:

We have included Western blot data for UBR5 and MARCHF7 knockdown efficiencies. For other factors where specific antibodies were unavailable, we followed your suggestion and provided graphical representations in the Appendix-figure S1, illustrating the siRNA target regions and qPCR target sites to confirm knockdown specificity and efficiency.

> *(3) In Figure 4 A: Write details on how this IP was done. What was the transfection time of this plasmid? Is the transfection time different from that of NSP16 in Figure 1A which shows a significant degradation of NSP16? Please discuss this in detail. It is recommended that this IP be done in +/- MG132. Since you have used siRNA and performed an IP, It is recommended to repeat the IP (with +/- MG132) using the MARCHF7 and UBR5 plasmids*

Thank you for your detailed review and suggestions! We have addressed your concerns as follows:

On the specific protocol for the co-IP in Figure 3A:

The detailed protocol for the immunoprecipitation (IP) experiment is as follows: on day 1, cells were plated, and on day 2, we co-transfected nsp16 and Ub expression plasmids. After 32 hours of transfection, we treated the cells with MG132 for 16 hours, then harvested the cells for IP. We included MG132 treatment in all ubiquitination IP experiments because, without MG132, nsp16 would be degraded, preventing us from observing changes in ubiquitination levels. We apologize for not clearly labeling this in the figure, and we have made the necessary modifications.

On the use of MG132 and NSP16 degradation:

Following your suggestion, we have clarified the use of MG132 in the IP experiments, which differs from the degradation of nsp16 shown in Figure 1A. In Figure 1A, we show the degradation of nsp16 in the absence of MG132 treatment.

On the overexpression of UBR5 and MARCHF7:

The effect of overexpressing UBR5 or MARCHF7 on ubiquitination has been validated in Figure 4 supplement 2. In these experiments, we explored the effect of UBR5 activity domain inactivation on nsp16 ubiquitination, as well as the effect of MARCHF7 truncation on nsp16 ubiquitination modification. In these experiments, overexpression of the wild-type E3 ligases was also included, and the results yielded the same conclusions as those from the E3 knockdown experiments, thereby validating the robustness of our findings.

> *(4) In Figure 4C: Appropriate controls are missing. The authors claim NSP16 is ubiquitinated and degraded by UBR5 and MARCHF7 via K27 and K48 chains. There is no NSP16 Only control. We cannot compare the NSP16 without an NSP16 transfection. I will suggest the authors repeat these individual controls in both the presence and absence of MG132.*

Thank you for your careful review and valuable suggestion! In response to your comment, we have redesigned the experiment and added a control group without nsp16 transfection. We have repeated the validation in the presence of MG132. Without MG132 treatment, nsp16 is degraded, leading to very low protein levels, making it difficult to observe the

phenomenon. We have updated the figure accordingly and made the necessary adjustments based on your suggestion (Figure 3E-F).

> *(5) In my opinion, the Figure 8 needs modification. It is requested to show the levels of strand-specific viral mRNA under UBR5 and MARCHF7 knock-down in +/- of MG312. This figure should also be supported by WB indicating the level of NSP16 (capping activity) and any of the viral proteins. This may validate that if the capping activity is lost, viral translation is affected and hence there is a reduction in virus titre. Alternatively, the figure can be modified by putting a sub-heading box over 7mGppA-RNA section and marking it as a future direction/ hypothesis.*

Thank you for your thorough and thoughtful review! Regarding the modification of Figure 8, we completely agree with your suggestion. Currently, examining the impact of viral RNA cap modification is technically challenging for us. Therefore, we have followed your advice and marked the investigation of how nsp16 degradation affects viral RNA cap structures as a future direction/hypothesis in the schematic of Figure 8. This revision helps provide direction for future experiments and enhances the clarity of the figure. Thank you for your thoughtful consideration and valuable suggestion!

> *Minor points:*
>
> *(1) Figure 2A: Align NSP16 Blot to actin.*

Thank you for your constructive feedback! We have redesigned the experiment and included an MG132 treatment group in Figure 2A. Consequently, the figure has been revised comprehensively, and the nsp16 blot has been aligned with tubulin.

> *(2) Figure 2C: It is recommended to properly align the lanes where the pLKO and shRNA labelling are overlapping.*

Thank you for your thoughtful suggestion! We have revised Figure 2C based on your recommendation to ensure that the pLKO and shRNA labeling no longer overlap. We sincerely apologize for any confusion this may have caused and appreciate your understanding and support.

> *(3) Just a curious question, what happens if we silence both UBR5 and MARCHF7 and check for virus titre? This is an additional work, but if the authors do not agree, it is ok.*

Thank you for your valuable suggestion! Regarding your question about silencing both UBR5 and MARCHF7, we indeed attempted to generate knockout cell lines, but unfortunately, we were not successful at this stage. We plan to explore alternative methods to establish stable knockout cell lines in our future experiments. Meanwhile, as shown in Figure 5 supplement 1, we have performed experiments where both UBR5 and MARCHF7 were knocked down simultaneously, followed by infection with virus-like particles. The results indicate that dual knockdown further enhances viral replication. These findings may partially address your question. Thank you again for your insightful suggestion!

https://doi.org/10.7554/eLife.102277.2.sa0